AD-A250 799

TECHNICAL REPORT BRL-TR-3337

BRL

CONDENSED-PHASE PROCESSES DURING SOLID PROPELLANT COMBUSTION. PART II: CHEMICAL AND MICROSCOPIC EXAMINATION OF CONDUCTIVELY QUENCHED SAMPLES OF RDX, XM39, JA2, M30, AND HMX-BINDER COMPOSITIONS

MICHAEL A. SCHROEDER
ROBERT A. FIFER
MARTIN S. MILLER
ROSE A. PESCE-RODRIGUEZ
GURBAX SINGH

DTIC
ELECTE
MAY 28 1992
S B D

MAY 1992

U.S. ARMY LABORATORY COMMAND

BALLISTIC RESEARCH LABORATORY
ABERDEEN PROVING GROUND, MARYLAND

92 5 27 066

92-13993

REPORT DOCUMENTATION PAGE

Public reporting burden for this collection of information is estimated to average 1 hour per response, including the time for reviewing instructions, searching existing data sources, gathering and maintaining the data needed, and completing and reviewing the collection of information. Send comments regarding this burden estimate or any other aspect of this collection of information, including suggestions for reducing this burden, to Washington Headquarters Services, Directorate for Information Operations and Reports, 1215 Jefferson Davis Highway, Suite 1204, Arlington, VA 22202-4302, and to the Office of Management and Budget, Paperwork Reduction Project (0704-0188), Washington, DC 20503.

1. AGENCY USE ONLY (Leave blank)	2. REPORT DATE	3. REPORT TYPE AND DATES COVERED
	May 1992	Final, November 1989–October 1990

4. TITLE AND SUBTITLE
Condensed-Phase Processes During Solid Propellant Combustion.
Part II: Chemical and Microscopic Examination of Conductively Quenched
Samples of RDX, XM39, JA2, M30, and HMX-Binder Compositions

5. FUNDING NUMBERS

PR: 1L161102AH43

6. AUTHOR(S)

Michael A. Schroeder, Robert A. Fifer, Martin S. Miller,
Rose A. Pesce-Rodriguez, and Gurbax Singh

7. PERFORMING ORGANIZATION NAME(S) AND ADDRESS(ES)

8. PERFORMING ORGANIZATION REPORT NUMBER

9. SPONSORING/MONITORING AGENCY NAME(S) AND ADDRESS(ES)

U.S. Army Ballistic Research Laboratory
ATTN: SLCBR-DD-T
Aberdeen Proving Ground, MD 21005-5066

10. SPONSORING/MONITORING AGENCY REPORT NUMBER

BRL-TR-3337

11. SUPPLEMENTARY NOTES

12a. DISTRIBUTION/AVAILABILITY STATEMENT

Approved for public release; distribution is unlimited.

12b. DISTRIBUTION CODE

13. ABSTRACT (Maximum 200 words)

Burning propellant samples were quenched, and the burned surfaces were examined microscopically and by chemical analysis. Studies are in progress on a series of propellants including XM39, M30, JA2, RDX, and HMX-polyester compositions. The results to date are consistent with the idea that at least at low pressures (below 2.0 MPa), a liquid layer forms during combustion of most of the propellants, with the possible exception of JA2; scanning electron microscope examination shows the existence of a liquid layer but does not provide evidence of degradation below this layer. The effect of composition and pressure on this liquid layer is discussed. Further gas chromatography mass spectrometry analysis confirms our earlier result that at least in the case of XM39, the stabilizer is depleted considerably in the surface layers, presumably by reaction with nitrogen oxides formed by decomposition of RDX and NC. Further high performance liquid chromatography results confirm our earlier result that for XM39, HMX2, and RDX (which contain the cyclic nitramines HMX and RDX), there is a significant increase in concentration of the mechanistically significant nitrosoamines MRDX and DRDX over the very small amounts possibly present as impurities in RDX and HMX. FTIR-PAS results provide evidence for condensed-phase reaction in M30 and JA2.

14. SUBJECT TERMS

solid propellants; gun propellants; quenching; combustion; propellants; HMX; RDX, JA2; M30; XM39; extinguishment

15. NUMBER OF PAGES
57

16. PRICE CODE

17. SECURITY CLASSIFICATION OF REPORT	18. SECURITY CLASSIFICATION OF THIS PAGE	19. SECURITY CLASSIFICATION OF ABSTRACT	20. LIMITATION OF ABSTRACT
UNCLASSIFIED	UNCLASSIFIED	UNCLASSIFIED	SAR

NSN 7540-01-280-5500

INTENTIONALLY LEFT BLANK.

TABLE OF CONTENTS

INTENTIONALLY LEFT BLANK.

LIST OF FIGURES

LIST OF TABLES

INTENTIONALLY LEFT BLANK.

ACKNOWLEDGMENTS

INTENTIONALLY LEFT BLANK.

1. INTRODUCTION

This is a progress report on work aimed at understanding the nature and importance of condensed-phase reactions in the combustion of solid nitramine and other gun propellants. Information on the nature and importance of condensed-phase reactions is needed as input for modeling studies. This information could also contribute to our understanding the relationship of chemical structure and of physical properties such as melting point, phase transition temperatures, etc., to explosive and propellant behavior.

Our initial work was described in a paper at the 1989 JANNAF Combustion meeting (Schroeder et al. 1989, 1990). Samples are obtained in either of the two following ways: 1) The propellants are burned in a low-pressure strand burner at different pressures of nitrogen; the sample is mounted on a massive copper block, and burning is interrupted by conduction of heat away from the burning surface as the burning surface approaches the copper block, as described by Novikov and Ryzantsev (1970); and 2) The propellant grains are ignited with a flame in air at ambient pressure; burning is interrupted by dropping the burning grain into a beaker of water. The previous report mainly emphasized preliminary results on XM39 and its ingredients; however, data have since been obtained on a series of burned samples including XM39, M30, JA2, RDX, and on HMX-polyester (HMX2) compositions; these data have been included in the present report. In the future, we plan to investigate quenching by rapid depressurization induced by breaking of a rupture disk in the strand burner; the various quenching methods will then be compared.

The samples are cleaved parallel to the grain axis and the cleaved surfaces examined with a scanning electron microscope (SEM). In addition, the surface layers are removed from the extinguished propellant grains by scraping them with a small, sharp knife. The scrapings are analyzed by spectroscopic methods such as gas chromatography-mass spectrometry (GCMS) and high performance liquid chromatography (HPLC). In addition, the unscraped surfaces are examined by Fourier transform infrared photoacoustic spectrometry (FTIR-PAS).

The literature contains a number of papers describing microscopic examination of "hot spots" in explosives and burned surfaces of propellant grains of HMX and compositions derived therefrom (Kubota and Sakamoto 1989; Derr et al. 1974; Derr and Boggs 1970;

1

Wilmot et al. 1981; Sharma et al. 1982, 1984, 1991; Mansour, Sharma, and Wilmot 1985; Sharma and Beard 1990a, 1990b; Zimmer-Galler 1968; Kubota 1981; Cohen-Nir 1981; Zhao and Zhao 1988; Stokes et al. 1989; Cohen, Stokes, and Strand 1989). There are also a number of papers describing chemical analysis of hot spots, and of the burned surface of nitrate ester propellants (Wilmot et al. 1981; Sharma et al. 1982, 1984; Hoffsommer, Glover, and Elban 1985; Mansour, Sharma, and Wilmot 1985; Sharma and Beard 1990a, 1990b). However, as far as we are aware, chemical analysis of burned surfaces has not been applied to nitramines or nitramine propellants; although in one study (Zimmer-Galler 1968) the surface layers of a quenched RDX-polyester composition were extracted with benzene and acetone, and the presence or absence of a residue under various conditions was noted. It was suggested that the variations in burning surface with particle size indicated an increase in surface temperature with decreasing particle size.

2. EXPERIMENTAL

Propellant and ingredient samples used were standard compositions. Lot numbers and grain descriptions were as follows: XM39, CI0885-200-1, cylindrical, 1/4 in × 1/4 in, 19-Perf.; M30, RAD-67878, cylindrical, 1/4 in × 5/8 in, 7-Perf.; and JA2, RAD-PDI-002-1F was received as unperforated, approximately 19-in-long sticks which were cut into cylindrical, 3/8-in diameter × 1/4 to 1/2-in-long grains that were used for the actual burns. The HMX2 composition (Vanderhoff 1988) was a composition containing 80% HMX and 20% polyester binder. It was received as sticks 4-in long and 1/4-in square, which were cut to lengths of approximately 1/4 in for the burns. RDX was Class-A RDX and was pressed into 1/2-in × 1/2-in cylindrical pieces of 91% theoretical maximum density; these pieces were further cut and shaped into approximately cylindrical ca. 1/4-in × 1/4-in pieces. The compositions of the propellants and formulations used are summarized in Table 1.

The samples were burned following one of a number of procedures; these included the following: 1) One end of the grain was ignited in air by contact with a candle, the burning end was allowed to burn for several seconds, and the grain was dropped into water; 2) The grain was attached to a massive copper stub, ignited in a strand burner under nitrogen, and allowed to burn down to the copper stub; as the burning surface approached the copper stub,

quenching occurred as a result of conduction of heat away from the burning grain by the copper stub, as described by Novikov and Ryzantsev (1970). In addition, we obtained several samples of XM39 which had, for unknown reasons, extinguished spontaneously while being burned in the strand burner at a pressure of 1.0 MPa under nitrogen.

Whenever the remaining portions of the grains were substantial enough to allow it, the burned grains were cooled to dry ice temperatures and split with a knife blade held vertical by mechanical means; when this knife was rested against the propellant grain and struck with a hammer, a clean split could be obtained (the knife was mechanically prevented from penetrating more than a small fraction of the grain). One half of the split grain was preserved intact for microscopic examination, and the surface layers of the other piece were removed by scraping with a small knife. Most of the grains burned under pressure with copper-block quenching (method 2 in the previous paragraph) were burned down to wafers only 100- or 200-μm thick. In these cases, part of the horizontal cross section of the wafer was cut with a knife, and the remaining part was separated with tweezers; the pulled-apart portion revealed enough of the vertical cross section to provide useful information.

The acetone-soluble portions of the scrapings were analyzed by GCMS and HPLC. Unscraped burned surfaces were examined by photoacoustic Fourier-transform infrared spectroscopy (PA-FTIR). The HPLC apparatus was a Perkin-Elmer Series 4 fitted with a C-18 column and interfaced to an LC-85 spectrophotometric UV detector operating at 254 nm. Injection solvent was acetone, and the eluant was 3:1 water-methanol. The GCMS apparatus consisted of a Hewlett-Packard 5970 mass selective detector (MSD) coupled to a Hewlett-Packard 5890 gas chromatograph containing an Alltech column of the following description: 30-m long, 0.25-μm i.d., Heliflex, Bonded FSOT, RSL-150, Stock No. 13639. The carrier gas was helium. The oven program was as follows: initial hold time—3 min at 50° C; heat to 225° C at 35° C/min; hold 15 min at 225° C.

Photoacoustic FTIR spectra were obtained on a Mattson Sirius 100 spectrometer using a MTEC 100 photoacoustic cell. The velocity of the interferometer moving mirror was 0.316 cm/s. All spectra were obtained after thoroughly purging the photoacoustic cell with helium. Spectra were measured at 8 cm^{-1} resolution and are the result of 32 co-added scans.

Single-beam spectra were ratioed to the photoacoustic spectrum of finely powdered carbon black.

The SEM used was a JEOL Model JSM-820 instrument. X-ray fluorescence (XRF) spectra were obtained using a Kevex model 3600-0374 x-ray fluorescence detector interfaced to a Kevex Delta Class Analyzer, running Kevex Quantex software, version V.

3. RESULTS

Typical HPLC and GCMS chromatograms for XM39 propellant are shown in our previous report (Schroeder et al. 1990); those are typical of the chromatograms for HMX2, RDX, M30, and JA2 obtained in the course of the work described in the present report.

HPLC peak area ratios for RDX, its mononitrosoamine (hexahydro-1,3-dinitro-5-nitroso-triazine [MRDX]) and its dinitrosoamine (hexahydro-1,3-dinitroso-5-nitro-triazine [DRDX]) are given in Table 2 for burned and unburned samples of XM39 propellant, pure RDX, and HMX2. This table also includes peak areas ratios for an unknown peak referred to as NHMX(?), which, based on its retention time relative to HMX (present as impurity in the RDX), could possibly be a nitrosoamine arising from replacement of one or more nitro groups of HMX by nitroso; however, in the absence of data on an authentic sample, the peak should be considered unidentified. For the sake of completeness, Table 2 also includes HPLC data from our previous report (Schroeder et al. 1989, 1990).

Tables of GCMS peak areas for stabilizer (diethyl centralite) and plasticizer (ATEC) from XM39 burned-layer scrapings and of unburned XM39 are given in Table 3; this table also includes stabilizer-plasticizer area ratios. For the sake of completeness, Table 3 also includes GCMS data from our previous report (Schroeder et al. 1989, 1990).

Several unknown peaks were also observed in the HPLC and GCMS chromatograms; these peaks were usually quite weak, but nevertheless seem worth mentioning. The HPLC and GCMS unknown peaks are summarized in Tables 4 and 5, respectively.

Typical photoacoustic FTIR spectra of unscraped, burned surfaces and of unburned samples of XM39, HMX2, RDX, M30, and JA2 are given in Figures 1–9. Because of the manner in which FTIR-PAS spectra are obtained, these figures show the actual spectra of the surface layers of the samples.

Typical SEM photographs of the burned surfaces of quenched and cleaved samples of XM39, HMX2, RDX, M30, and JA2 are shown in Figures 10–21. A summary of observations based on such photographs is presented in Table 6.

X-ray fluorescence spectra of the burned samples of XM39 showed the presence of traces of potassium and calcium. These elements sometimes occur as impurities in graphite, and so may have been present as impurities in the graphite coating on the XM39 grains. The burned samples of RDX did not show the presence of any elements other than carbon, oxygen, and nitrogen. The burned samples of HMX2 showed the presence of small amounts of aluminum and calcium as well as sodium and calcium in some cases. JA2 showed weak peaks from calcium, magnesium, and sulfur in its XRF spectrum. The burned sample of M30 did not show the presence of any elements other than carbon, nitrogen, and oxygen.

4. DISCUSSION

4.1 HPLC Results. The burned-layer scrapings from both compositions (XM39 and RDX) containing the nitramine RDX exhibited HPLC peaks that are believed, on the basis of their retention times, to be the nitrosoamines derived from RDX by replacement of one (MRDX) or two (DRDX) nitro groupings by nitroso (Table 2). (The trinitroso derivative hexahydro-1,3,5-trinitroso-1,3,5-triazine [TRDX] was apparently not formed in amounts detectable by our methods.) In agreement with this, these nitrosoamines have been detected in residues from thermal decomposition (Hoffsommer and Glover 1985; Fifer et al. 1985) and drop-weight impact testing (Hoffsommer, Glover, and Elban 1985), although as far as we are aware our previous report (Schroeder et al. 1989, 1990) was the first time they have been detected from propellant combustion. Since the response factors for these compounds are similar (Fifer et al. 1985; Hoffsommer, Glover, and Elban 1985), the relative intensities in Table 2 should provide rough, order-of-magnitude estimates of the amounts of nitrosoamines formed, relative

to HMX and RDX. It is thus estimated that the nitrosoamines are present in amounts as high as 10–20% of the unreacted HMX and RDX in some cases.

In addition, the compositions containing the nitramine HMX exhibited a rather weak peak with a retention time slightly lower than that of HMX. Possibly this peak is due to a nitrosoamine derivative of HMX.

The formation of nitrosoamines in amounts as large as these near the burning surface of nitroamine propellants and compositions seems quite significant with regard to chemical mechanisms; this will be discussed later under Section 5. In addition to the mechanisms discussed there, another possibility arises from the occurrence (Rauch and Colman 1970) in at least some samples of unburned RDX and of GC peaks with the same retention times as MRDX and TRDX consistent with the presence of these materials as trace impurities. Since MRDX decomposes about 10% more slowly than RDX at 180° C in benzene under pressure (Hoffsommer and Glover 1985), it is difficult to rigorously rule out the possibility that trace amounts initially present could accumulate to larger concentrations at the burning surface. Even though we did not detect any nitrosoamines in the lots of XM39, RDX, and HMX used in the present work, the possibility of the presence of amounts too small to detect by our methods should be kept in mind.

Several trends were observed in the HPLC data (Table 2). First, there seems to be a tendency for the runs at 2.0 MPa (the highest pressure used) to show less nitrosoamine content, in other words, to resemble the unburned material more than the runs at lower pressures. This may well result from faster combustion and a resulting tendency to spend less time in the liquid layer at higher pressures; however, although an attempt was made to scrape away only the liquid layer, there is still a possibility that the thinner liquid layers on the higher-pressure samples resulted in a higher proportion of unburned material in the scrapings. Second, the samples with highest nitrosoamine concentrations also have the highest HMX/RDX ratio; presumably, this enrichment results from a higher decomposition rate for RDX than for HMX under these conditions.

Also, it may be possible to get a degree of depth profiling by examining lines 13 and 14 of Table 2. These lines arose as follows: When the ambient-pressure RDX samples were

6

burned and put in water, material apparently from foam or liquid thrown off during combustion was noticed floating on the surface of the water. This was gathered and analyzed; it gave higher nitrosoamine levels than any other RDX sample. This thrown-off material presumably came from the outer edges of the liquid layer, and it seems unlikely that water alone could lead to formation of nitrosoamines from RDX. Therefore, its higher nitrosoamine concentration suggests that nitrosoamine concentrations may increase on going from the bottom to the top of the liquid layer.

In addition, the HPLC chromatograms contained a number of very weak, unknown peaks apparently corresponding to compounds formed in the condensed phase during combustion (Table 4). Attempts to identify these peaks are now in progress.

4.2 GCMS Results. The GCMS peaks from the chromatograms of burned-layer scrapings from burned samples of XM39 suggested an interesting conclusion: In the melt layer, the level of stabilizer diethyl centralite (retention time 12.5 min) is decreased relative to the plasticizer ATEC (retention time ca. 16.0 min) from the levels found in unburned XM39. This is illustrated in Table 3, which shows peak areas for the stabilizer and plasticizer, together with the ratio of these two peaks for each run. This trend, which was reported in our previous write-up (Schroeder et al. 1989, 1990), has since been substantiated by further observation. However, it was not possible to verify this conclusion for the diethyl centralite stabilizer in M30 propellant or the Akardit II (dimethyl centralite) stabilizer in JA2 due to lack of a stable (on the GC column) reference material such as acetyltriethylcitrate (ATEC) with which to compare them.

Possibly this decrease in stabilizer relative to plasticizer is due to removal of stabilizer by nitrogen oxides generated during combustion, by mechanisms similar to those involved in shelf-life stabilization of the propellant by removal of trace amounts of nitrogen oxides and acids. In other words, nitrogen oxides generated during combustion react with the stabilizer and remove it.

Note that there seems to be less stabilizer depletion in the higher pressure (2.0 MPa) runs. Note also that a similar trend with regard to nitrosoamine formation was described in the previous section. These trends may well result from faster combustion and a resulting

7

tendency to spend less time in the liquid layer at higher pressures. However, it should be remembered that although an attempt was made to scrape away only the liquid layer, it is possible that the thinner liquid layers on the higher-pressure samples resulted in a higher proportion of unburned material in the scrapings.

In addition, the GCMS chromatograms contained a number of very weak, unknown peaks apparently corresponding to compounds formed in the condensed phase during combustion (Table 5). Attempts to identify these peaks are now in progress.

4.3 FTIR-PAS Results.

4.3.1 XM39. As described previously (Schroeder et al. 1989, 1990), the results of FTIR-PAS studies on burned and unburned samples of XM39 suggest that the burned surface includes a higher proportion of cellulose acetate butyrate (CAB) and/or polymeric decomposition product than does the unburned XM39.

4.3.2 HMX2. Figures 1–3 show FTIR-PAS spectra of burned and unburned samples of HMX2 (80% HMX and 20% polyester binder). The only signs of the polyester in the spectrum of the unburned sample (Figure 1) are the carbonyl band at 1,720 cm^{-1} and three other smaller bands, one at 1,025 cm^{-1} and two near 700 cm^{-1}; the remaining polyester bands are obscured by HMX bands. These bands are larger in the spectrum of the burned HMX2 (Figures 2 and 3) than in the spectrum of unburned HMX2 (Figure 1).

4.3.3 M30. Figures 4–6 show the FTIR-PAS spectra of burned and unburned samples of M30. The spectrum of the unburned sample is shown in Figure 4. Comparison of this spectrum with that of burned material (Figures 5 and 6) reveals that the principal difference is a band at about 2,160 cm^{-1}. Since this band is not observed in the spectra of burned JA2, which also contains nitrocellulose and nitroglycerine, we believe that it is related to nitroguanidine (NQ) decomposition. Absorption in this region is consistent with sp-hybridized materials such as nitriles, isonitriles, azides, alkynes, etc.; of these, the ones that seem offhand to make the most sense chemically (Stals and Pitt 1975; Lee and Back 1988) are cyanamide (H_2N-CN) or a substituted cyanamide such as nitrocyanamide (O_2N-NH-CN) or dicyandiamide ($[H_2N]_2C$=N-CN) (possibly formed by dimerization of cyanamide).

8

4.3.4 JA2. Figures 7–9 show the FTIR-PAS spectra for unburned (Figure 7) and burned (Figures 8 and 9) samples of JA2 propellant. This formulation contains three components that are structurally related (NC, NG, and DEGDN), making interpretation of spectra difficult. Considering that approximately 40% of the formulation is small plasticizer molecules that are likely to evaporate or decompose more readily than nitrocellulose, it seems reasonable to suppose that FTIR-PAS spectra of burned JA2 propellant will be dominated by nitrocellulose, which accounts for the remaining 60% of the formulation.

The main features of the spectra of the burned JA2 samples are the appearance of a band at 1,730 cm^{-1} and the relative decrease of the NO_2 symmetric and asymmetric stretching bands (1,650 and 1,280 cm^{-1}, respectively) relative to the C-O-C stretching bands (1,200 to 950 cm^{-1}) (compare Figure 7 with Figures 8 and 9).

One possible explanation for these changes is that carbonyl groups are generated from loss of NO_2 from nitrocellulose; the large relative intensity of the C-O-C bands indicates that most of the nonenergetic cellulose backbone remains intact. This explanation is consistent with earlier reports (Fifer 1984) that one carbonyl group forms for each nitrate group that is lost and that secondary reactions in the condensed phase do not lead immediately to degradation of the glucose ring of nitrocellulose.

It has been reported (Sharma et al. 1984, 1991) that x-ray photoelectron spectroscopic analysis of the surface of a burned, depressurization-quenched sample of a double-base propellant (U.S. Navy N5 Propellant) suggested the presence of nitrite esters and of an oxime-like material. Our results (Figures 7–9) are inconclusive with regard to the presence of these materials in the closely related JA2 propellant. Examination of the spectra of the burned samples (Figures 8 and 9) for the nitrite ester absorption at 1,600–1,650 cm^{-1} and 775–830 cm^{-1} (Silverstein, Bassler, and Morrill 1981) is inconclusive because of the small amount of nitrite ester suggested by Figure 1 of Sharma et al. (1984) (Figure 3 of Sharma et al. [1991]). Examination for the oxime absorptions at 1,650–1685 cm^{-1} (weak) and 930–960 cm^{-1} (strong) (Gordon and Ford 1972) is inconclusive because of a) the presence of strong nitrate-ester absorption in the former region and b) the fact that the latter region lies in a valley between two strong peaks in the spectrum (Figure 7) of the unburned JA2 propellant; this valley "fills up" in the spectra of the burned samples (Figures 8 and 9), but no actual peak is evident.

9

4.3.5 Pressure Effects. In some cases, there seems to be a tendency for the effects mentioned previously (Sections 4.3.1–4.3.4) to be accentuated by pressure. Due to the possibility of interference by other effects such as buildup of undecomposed binder with time, this tendency should not be overemphasized and is under further investigation.

4.4 SEM Examination of Burned Propellant Samples. SEM photographs of quenched, cleaned surfaces of burned samples are shown inn Figures 10–21. A summary of observations from such photographs is presented in Table 6.

4.4.1 XM39. Observations are summarized in Table 6. Our previous report (Schroeder et al. 1989, 1990) included a number of SEM photographs of the burned, extinguished surfaces of samples of XM39 that had been burned in air at ambient pressure and extinguished by dropping them in water. These photographs indicated the presence of a liquid layer about 100–300 μm thick, with little, if any, evidence of degradation below this liquid layer.

SEM photographs were taken of samples of XM39 that had been burned in a strand burner at a pressure of 2.0 MPa. A cross section of the melt layer (Figure 10) appears to be noticeably thinner than when burned at atmospheric pressure. Pictures looking down onto the burned surface of the same grain show what appears to be crystallized RDX overlain by pieces of material that is presumably its binder or its decomposition products (Figure 11).

4.4.2 HMX2. SEM photographs were taken of burned samples of HMX2. One photo (Figure 12) shows a cross section of the burned surface of a piece of HMX2 burned in air at ambient pressure with water quenching. The presence of a liquid layer can be inferred from the smooth appearance of the top of the burned surface in the background; its thickness is difficult to evaluate but appears to be about 100 μm, noticeably thinner than the XM39 melt layer under the same conditions (Schroeder et al. 1989, 1990). In another view of the surface of the same sample (Figure 13), bubbles and crystallization can both be seen.

Another photo (Figure 14) shows a cross section of the burned surface of a grain of HMX2 burned at 0.5 MPa; this includes a grain (center) that appears to have been actually burning through at the surface when combustion stopped. The melt layer here was about 75 μm thick.

10

4.4.3 RDX. In an overview (Figure 15) of a grain of pure RDX that had been burned in air at ambient pressure and quenched by dropping it in water, the surface appears smooth, with protuberances that may be bubbles. It was difficult to estimate the depth of the melt layer, but from other photographs (not shown), it appeared to be about the same as for XM39 burned under the same conditions. Surprisingly, signs of crystallization were evident at only a few places on the surface of this grain. At higher pressures with copper quenching, RDX burned down so close to the copper block that the solid RDX melt layer structure was obliterated. Crystallization was evident (Figure 16) on the surface of pressed samples of RDX that were burned at these pressures (up to 0.5 MPa).

4.4.4 M30. On the surface of a grain of M30 that had been burned in air at ambient pressure and quenched with water, there is a very thin, bubbly melt layer which covers the surface completely (Figure 17). Below the surface, the grains of NQ can be seen to be oriented perpendicular to the surface. At higher pressures, the melt layer becomes thinner and finally reaches the point where it no longer covers the surface entirely, and the ends of the NQ crystals can be seen through the liquid layer (Figure 18).

4.4.5 JA2. The burned surfaces of samples of JA2 (Figures 19–21) burned in air at ambient pressure, then water quenched appeared either 1) uneven with signs of bubbles; or 2) relatively smooth, except for some cracks and unevenness, with an absence of bubbles (Figure 19). We do not understand the reason for the occurrence of the relatively smooth, bubbleless surface. At pressures of 0.5–2.0 MPa, the surface was uneven, and there were signs of bubbles (Figures 20 and 21). The liquid layer was so thin that it is hard to distinguish it in photographs of extinguished, sectioned grains of JA2. This is in agreement with the report (Sharma et al. 1984) that an unleaded double-base rocket propellant quenched by depressurization at 4.5 or 8.55 MPa exhibited a reaction zone only about 10 μm thick.

5. CONCLUSION

5.1 Physical Description of the Burned Surface. At the relatively low pressures used here, there appears to be a melt layer present on all of the formulations studied, with the possible exception of JA2, which differs from the others in that it doesn't have a crystalline oxidizer.

11

5.1.1 Effect of Composition on Thickness of Melt Layer. The melt layer seems to be thinner for the HMX composition HMX2 than for RDX and for the RDX composition XM39 (Table 6). This is in agreement with the previous literature (Derr et al. 1974; Derr and Boggs 1970; Wilmot et al. 1981; Sharma et al. 1982, 1984; Mansour, Sharma, and Wilmot 1985; Sharma and Beard 1990a, 1990b; Zimmer-Galler 1968; Kubota 1981; Cohen-Nir 1981; Zhao and Zhao 1988; Stokes et al. 1989; Cohen, Stokes, and Strand 1989). Of the compositions unambiguously showing a melt layer, the melt layer seems to be thinnest of all for the nitroguanidine composition M30 (Table 6).

5.1.2 Effect of Pressure on Thickness of Melt Layer. For the same formulation, there also seems to be a tendency for the thickness of the melt layer to decrease with pressure (Table 6). This is in agreement with the previous literature (Derr et al. 1974; Derr and Boggs 1970; Wilmot et al. 1981; Sharma et al. 1982, 1984; Mansour, Sharma, and Wilmot 1985; Sharma and Beard 1990a, 1990b; Zimmer-Galler 1968; Kubota 1981; Cohen-Nir 1981; Zhao and Zhao 1988; Stokes et al. 1989; Cohen, Stokes, and Strand 1989).

Probably the most dramatic illustration of this is provided by the nitroguanidine composition M30, the surface of which is completely covered at one atmosphere, but which has, after copper quenching at 2.0 MPa, the ends of the nitroguanidine crystals exposed in some places.

5.1.3 Presence of Bubbles. For most formulations at most pressures below 2.0 MPa, bubbles seem to be present.

5.2 Surface Chemistry.

5.2.1 Evidence for Condensed Phase Chemistry. There is evidence for condensed phase decomposition during combustion of all formulations studied, at least at the relatively low pressures employed in these experiments.

In the case of the cyclic nitramine compositions XM39, HMX2, and RDX, this evidence consists of the formation of nitrosoamines derived from the cyclic nitramine oxidizers RDX and HMX (Table 2).

In addition, in the case of XM39, evidence of condensed-phase decomposition is provided by the observed decrease in the ratio of stabilizer diethyl centralite to the plasticizer ATEC; this decrease is most easily explained by removal of stabilizer due to reaction with nitrogen oxides (NO and NO_2) generated by condensed-phase decomposition of the oxidizers RDX and nitrocellulose.

In the case of the conventional double- and triple-base propellants M30 and JA2, the evidence consists primarily of the appearance (see Section 4.3) in their infrared (FTIR-PAS) spectra of additional peaks due to apparent decomposition products. (Although JA2 is technically a triple-base propellant since it has three main constituents, its composition is chemically very close to the conventional [NC-NG] double-base propellants, since DEGDN and NG are both low-molecular-weight nitrate esters.) The peaks in question were primarily in the carbonyl region for JA2 and in the nitrile region for M30.

5.2.2 Possible Chemical Implications of Bubbles. As mentioned previously, for most formulations at most of the relatively low pressures employed in the present studies, bubbles appear to be present (Figures 10–22); possible exceptions to this appear to be JA2 burned at atmospheric pressure in air and 2.0 MPa. This could be important to modelers because of the possibility that gaseous products trapped in bubbles could be reacting at pressures and concentrations differing from those in the gaseous phase, with resulting local changes in composition of primary products and of temperature.

5.2.3 Chemical Mechanisms. Possible mechanisms for the case of the RDX composition XM39 were discussed in our previous report (Schroeder et al. 1989, 1990). These included stabilizer depletion due to reaction with nitrogen oxides generated during condensed phase decomposition and nitrosoamine formation by either 1) recombination between NO formed in the decomposition and the nitrogen-centered dinitro-RDX radical formed by $N-NO_2$; or 2) deoxygenation of the starting RDX by radical species formed in the decomposition. Possibility of mechanism 2 is indicated by the formation of nitrosamines with unbroken N-N bonds in the scrambling studies of Behrens (1989).

6. WORK NEEDED/FUTURE PLANS

The next phase of this work will involve carrying out runs in which quenching is by depressurization; the results obtained by the three quenching methods will then be compared. Also, optical examination of the burned surfaces will be carried out, particularly in view of the possibility that studies of color changes and variations may yield information on the occurrence (or lack thereof) of chemical changes in the solid below the liquid layer. Ways of obtaining improved depth profiling of the burned layers will also be explored; these include microabrasive blasting, microtoming, solvent dipping, and improved scraping procedures. Other propellant formulations will also be examined.

Isotope-scrambling studies on burning (rather than merely decomposing) samples are needed. These would involve use of recrystallized mixtures of unlabeled RDX or HMX with RDX or HMX labeled with nitrogen-15 in all nitrogens, both in the ring and in the nitro groups. Use of these mixtures would lead to scrambled nitrosoamines if the recombination mechanism were operating, but to unscrambled nitrosamines if the oxygen-abstraction mechanism was operating. Partial scrambling would mean that both mechanisms were operating to some degree. Note, however, that while formation of fully scrambled nitrosoamines would provide no evidence for oxygen abstraction, it would not necessarily rule it out, since the scrambling could have taken place by further N-N cleavage equilibria before or after formation of the nitrosoamines.
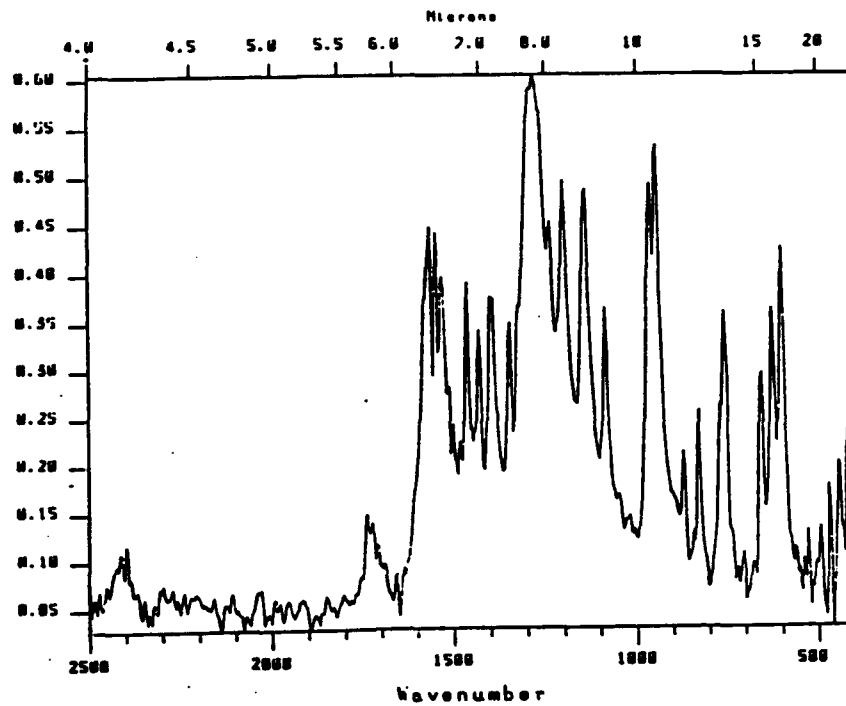
Figure 1. Photoacoustic FTIR Spectrum of Unburned HMX2 (Vertical, Intensity; Horizontal, Wavelength [Microns] or Frequency [cm⁻¹]).
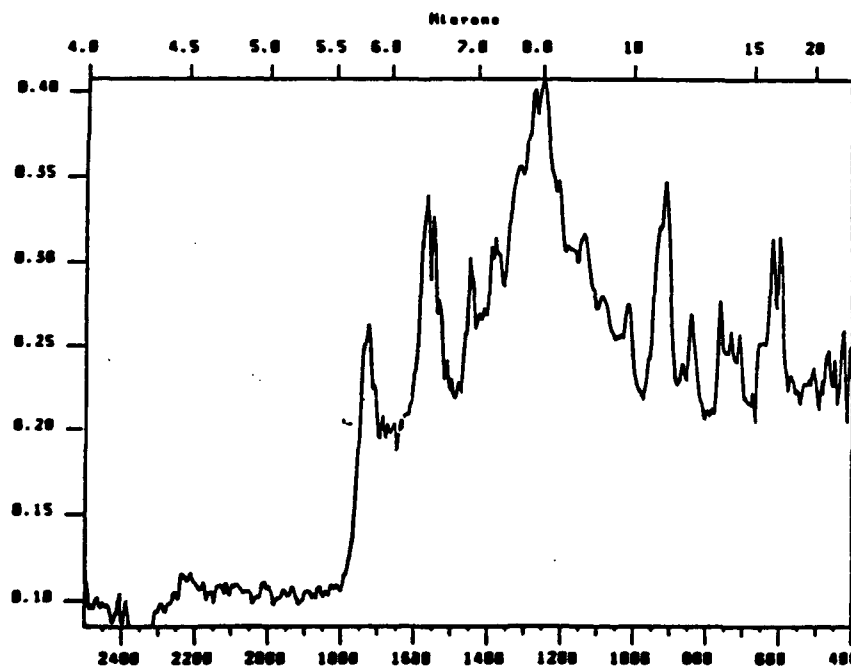
Figure 2. Photoacoustic FTIR Spectrum of HMX2 Burned at 1.0 MPa (Vertical, Intensity; Horizontal, Wavelength [Microns] or Frequency [cm⁻¹]).

15
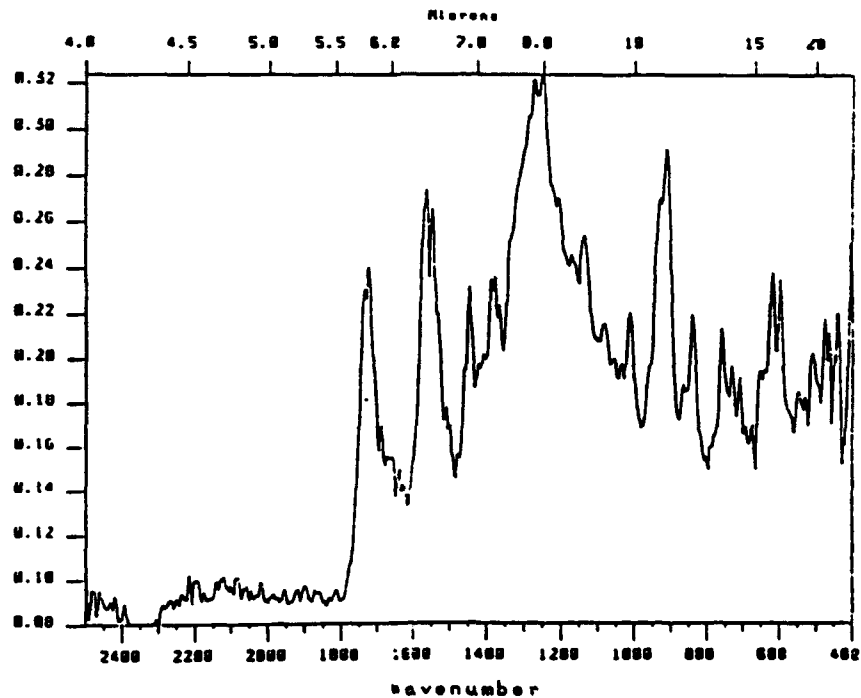
Figure 3. Photoacoustic FTIR Spectrum of HMX2 Burned at 2.0 MPa (Vertical, Intensity; Horizontal, Wavelength [Microns] or Frequency [cm^{-1}]).
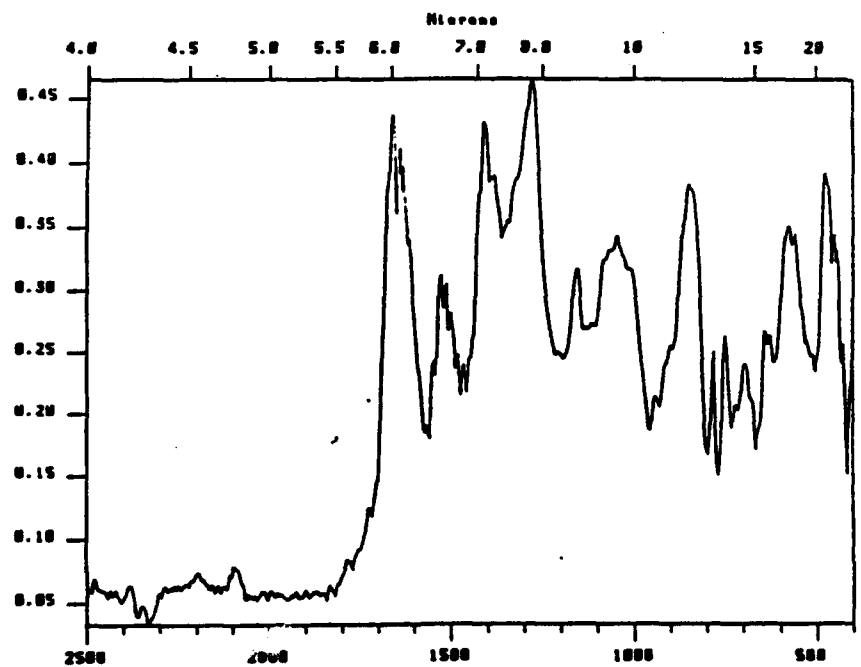
Figure 4. Photoacoustic FTIR Spectrum of Unburned M30 (Vertical, Intensity; Horizontal, Wavelength [Microns] or Frequency [cm^{-1}]).

16
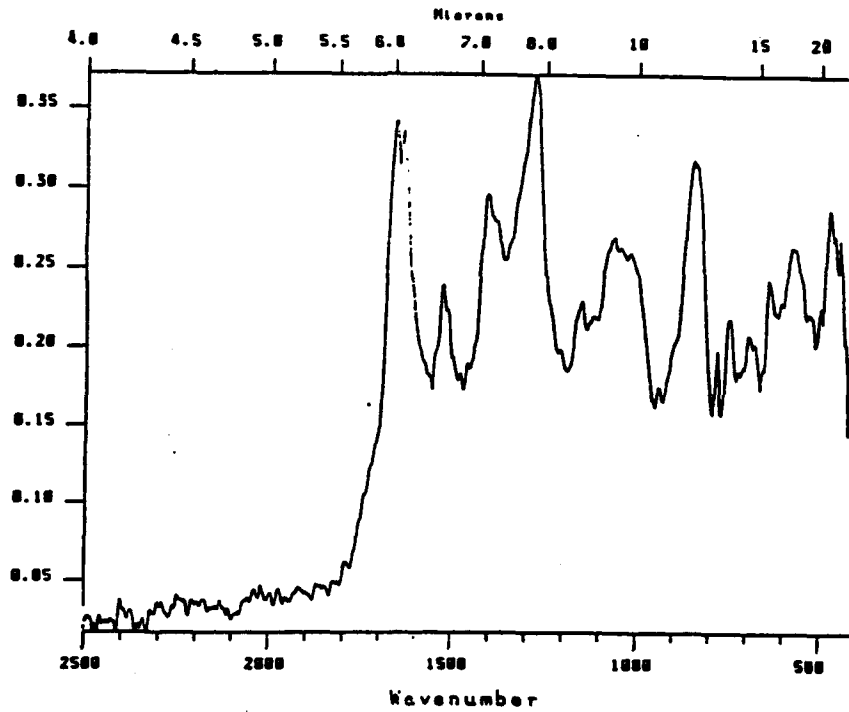
Figure 5. Photoacoustic FTIR Spectrum of M30 Burned at 0.5 MPa (Vertical, Intensity; Horizontal, Wavelength [Microns] or Frequency [cm^{-1}]).
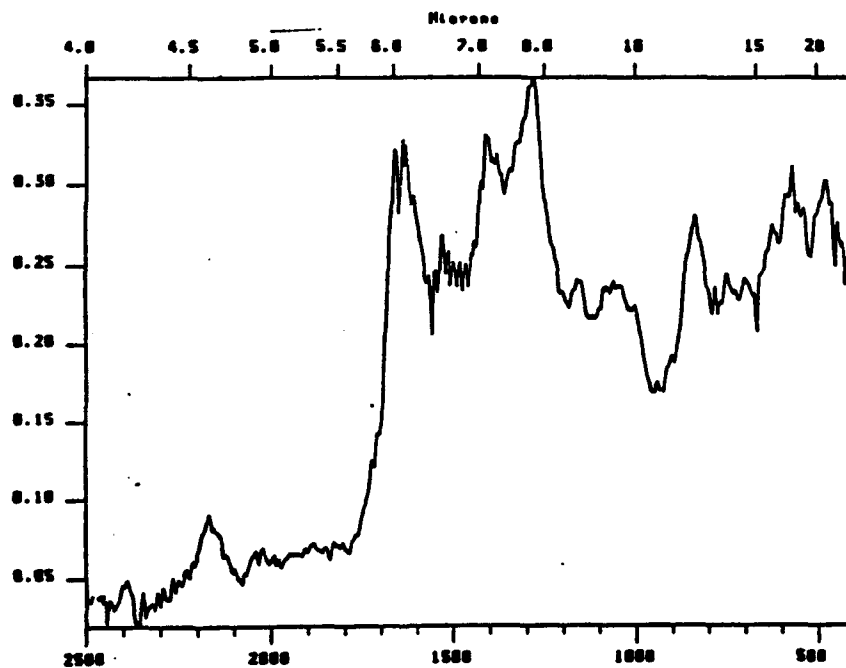
Figure 6. Photoacoustic FTIR Spectrum of M30 Burned at 2.0 MPa (Vertical, Intensity; Horizontal, Wavelength [Microns] or Frequency [cm^{-1}]).

17
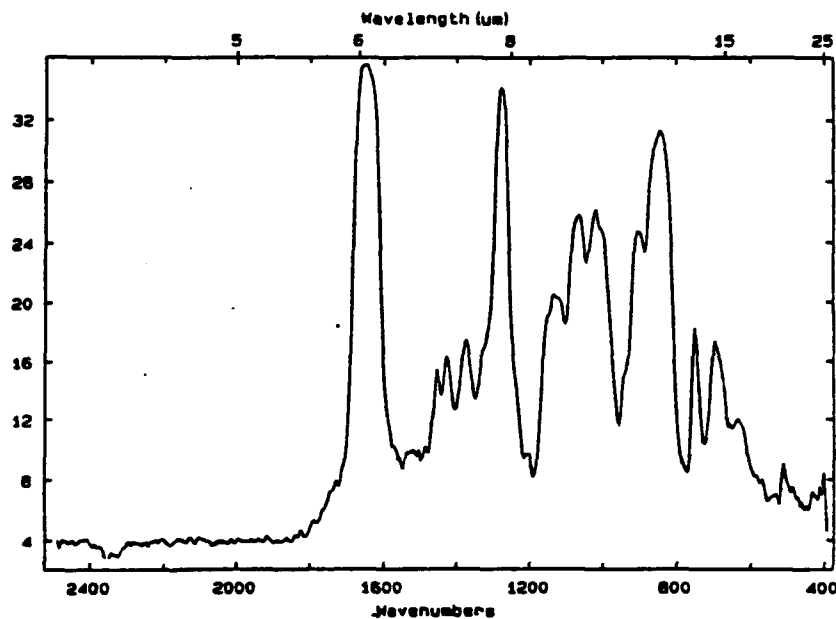
Figure 7. Photoacoustic FTIR Spectrum of Unburned JA2 (Vertical, Intensity; Horizontal, Wavelength [Microns] or Frequency [cm^{-1}]).
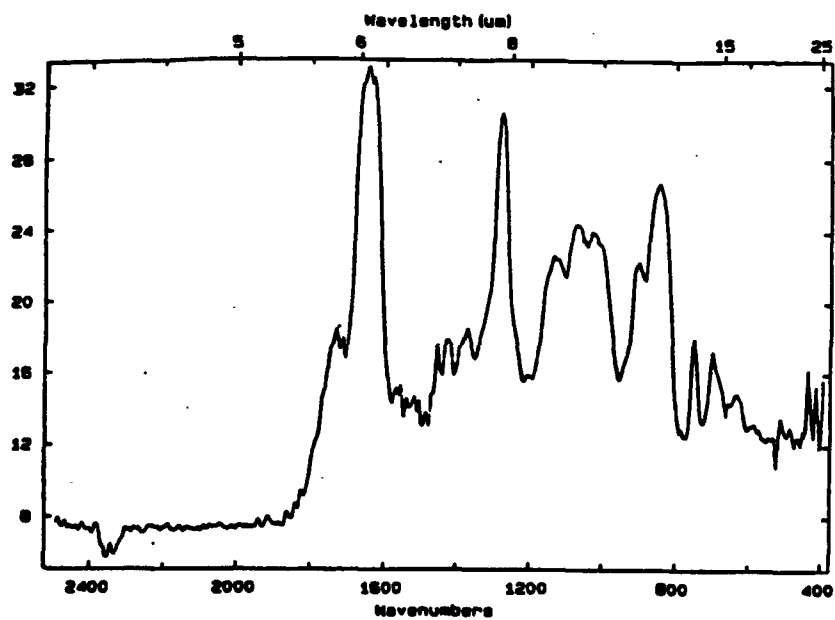
Figure 8. Photoacoustic FTIR Spectrum of JA2 Burned at Ambient Pressure (Vertical, Intensity; Horizontal, Wavelength [Microns] or Frequency [cm^{-1}]).
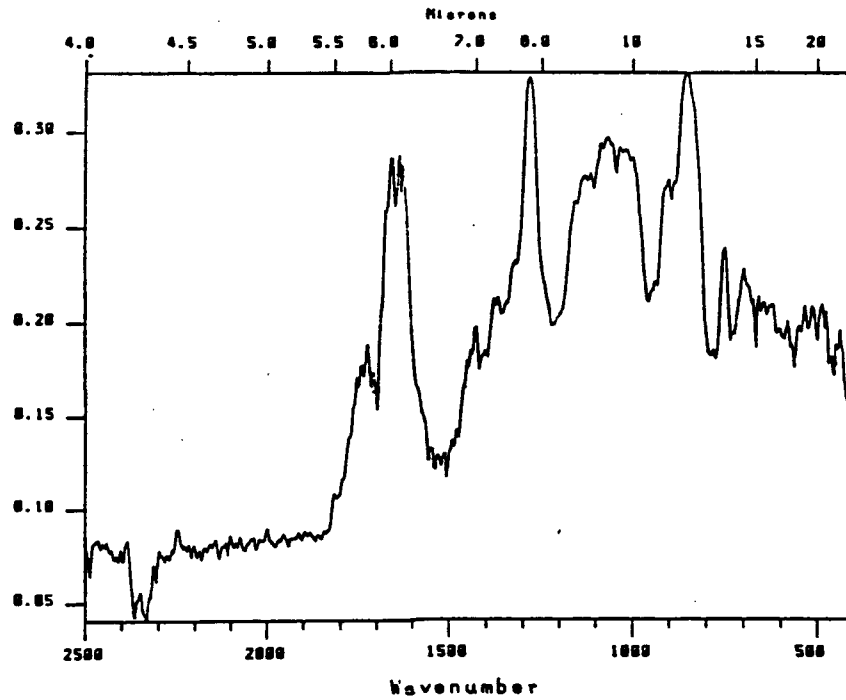
Figure 9. Photoacoustic FTIR Spectrum of JA2 Burned at 0.5 MPa (Vertical, Intensity; Horizontal, Wavelength [Microns] or Frequency [cm^{-1}]).
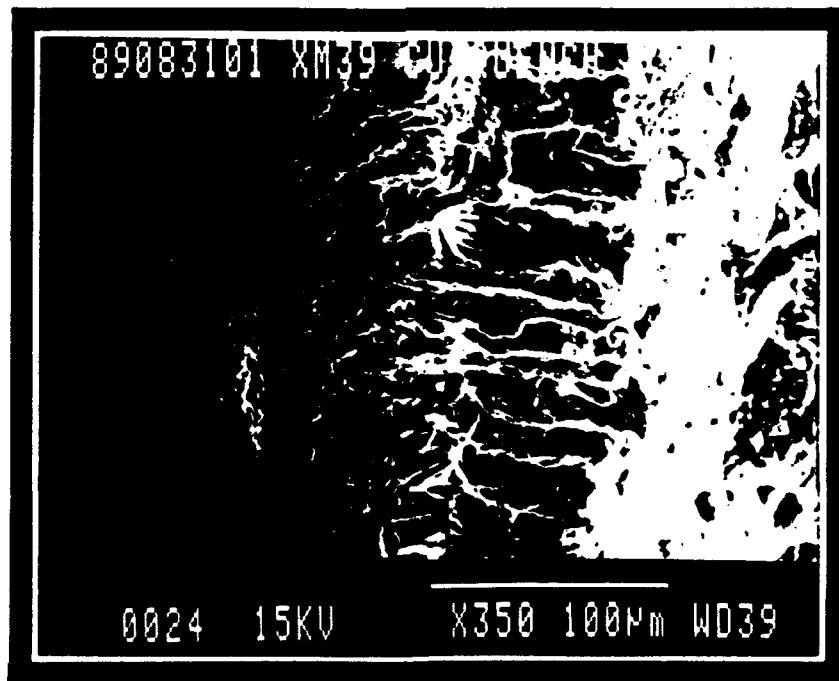
Figure 10. SEM Photograph (350x) of Cross Section of Burned Surface of XM39 (2.0 MPa, Copper Quenched).

Figure 11. SEM Photograph (370x) Burned Surface of XM39 (2.0 MPa, Copper Quenched).
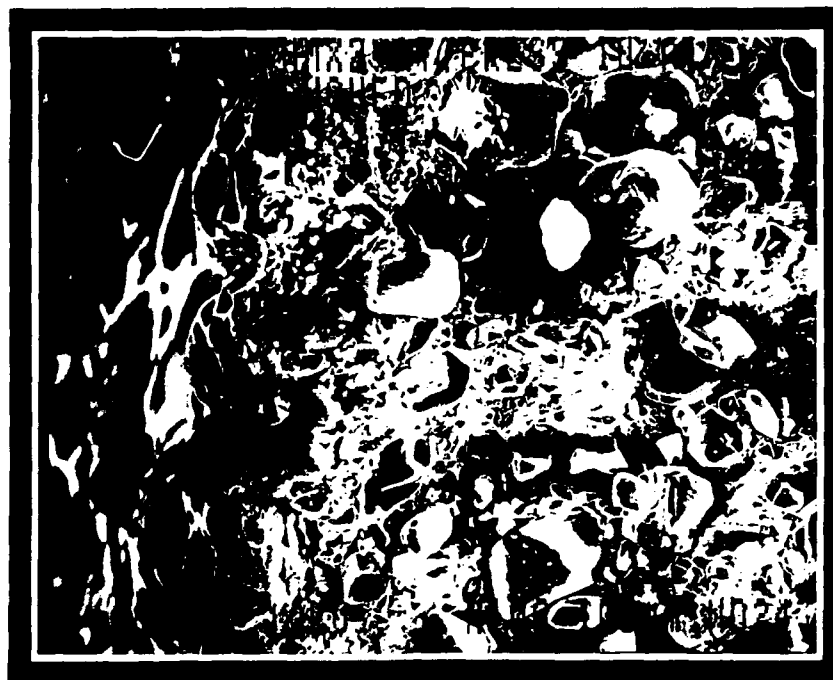
Figure 12. SEM Photograph (400x) of Cross Section of Burned Surface of HMX2 (Ambient Pressure, Water Quenched).
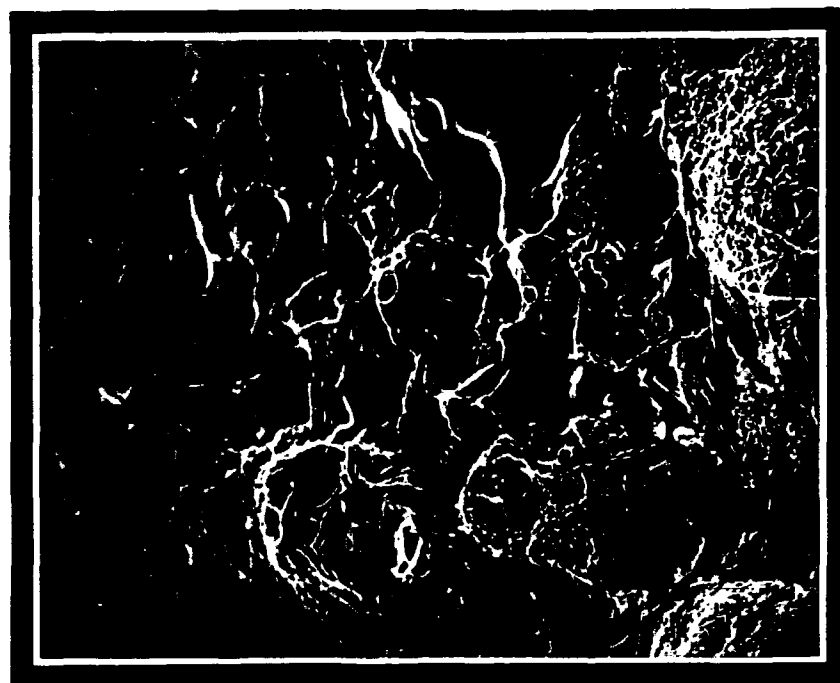
Figure 13. SEM Photograph (330x) of Burned Surface of HMX2 (Ambient Pressure, Water Quenched).

Figure 14. SEM Photograph (130x) of Cross Section of Burned Surface of HMX2 (0.5 MPa, Copper Quenched).
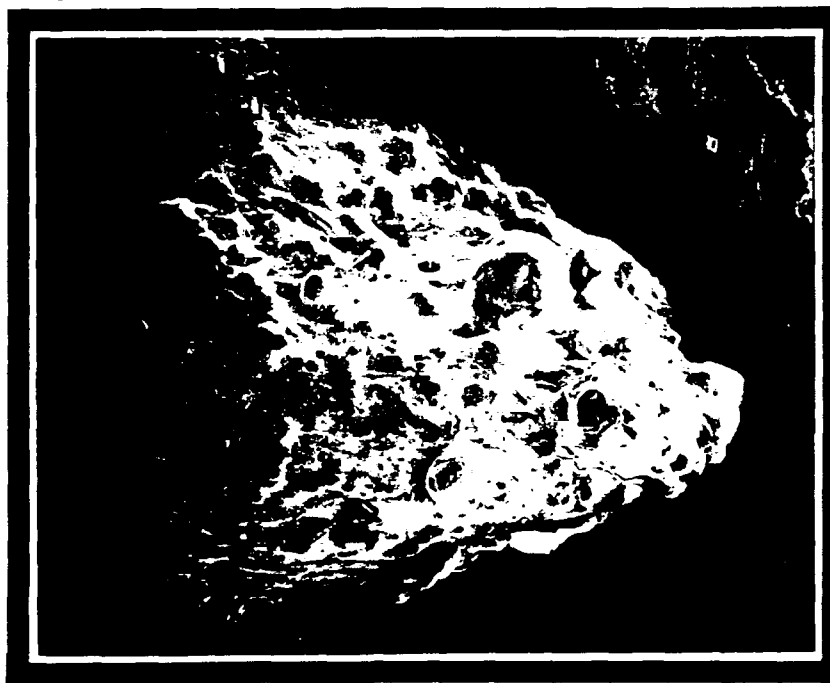
Figure 15. SEM Photograph (25x) of Burned Surface of RDX Grain (Ambient Pressure, Water Quenched).

Figure 16. SEM Photograph (370x) of Burned Surface of RDX Grain (0.5 MPa, Copper Quenched).
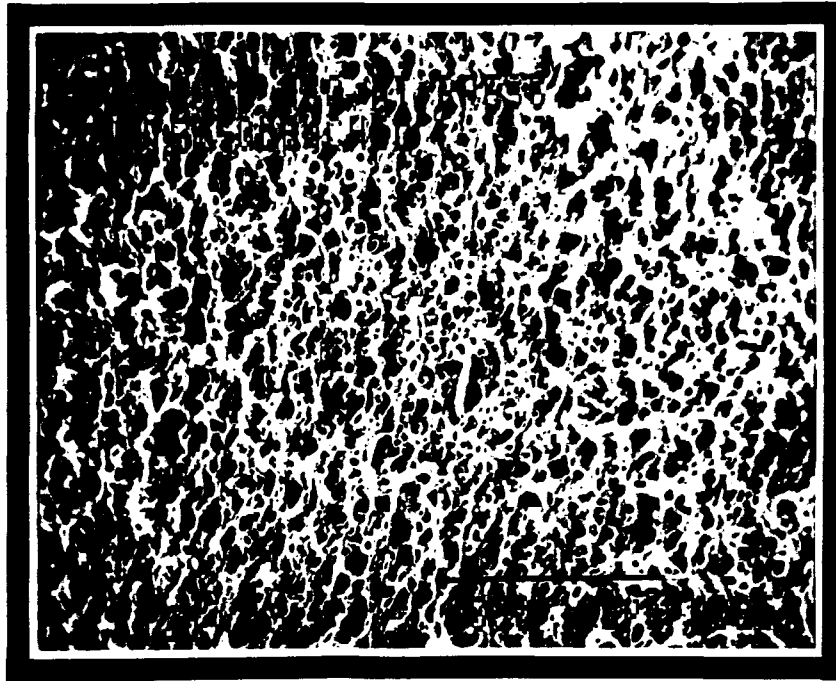
Figure 17. SEM Photograph (330x) of Burned Surface of M30 (Ambient Pressure, Water Quenched).
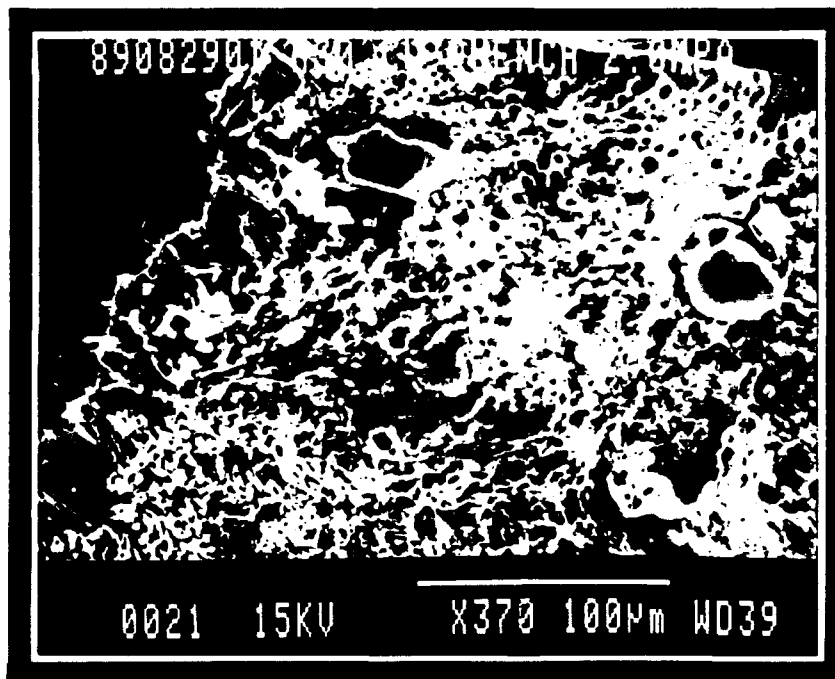
Figure 18. SEM Photograph (370x) of Cross Section of Burned Surface of M30 (2.0 MPa, Copper Quenched).

23
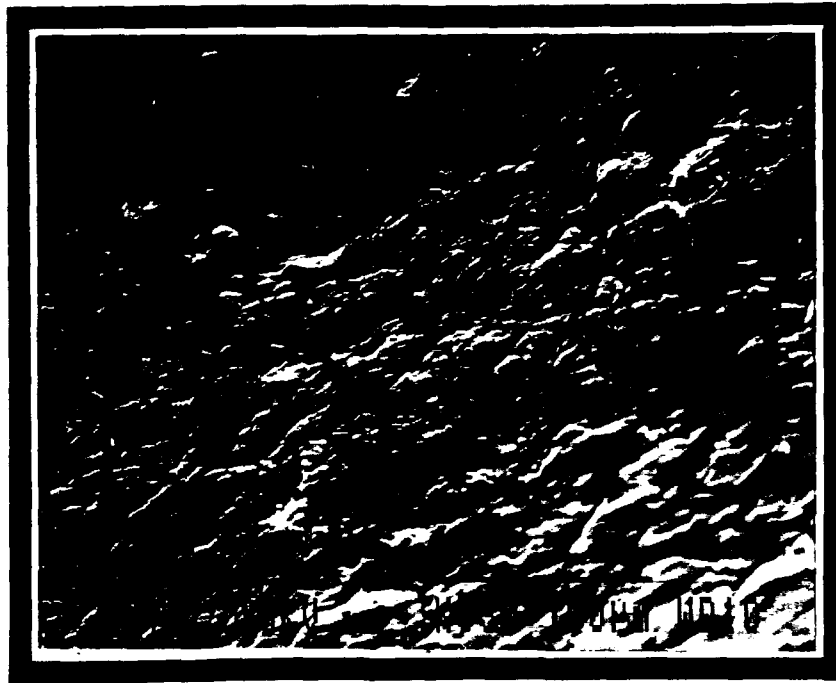
Figure 19. SEM Photograph (330x) of Burned Surface of JA2 Grain (Ambient Pressure, Water Quenched).
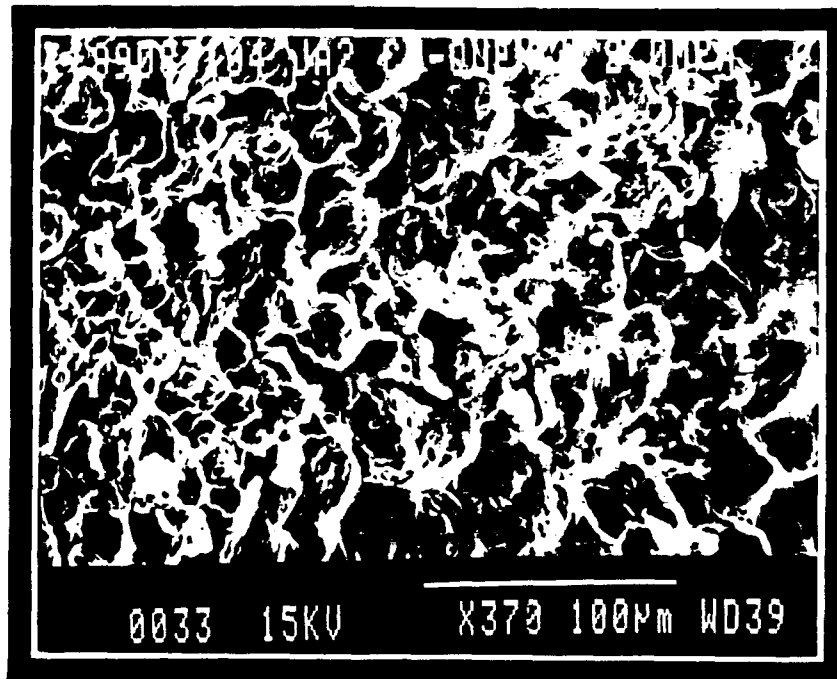
Figure 20. SEM Photograph (370x) of Burned Surface of JA2 (2.0 MPa, Copper Quenched).
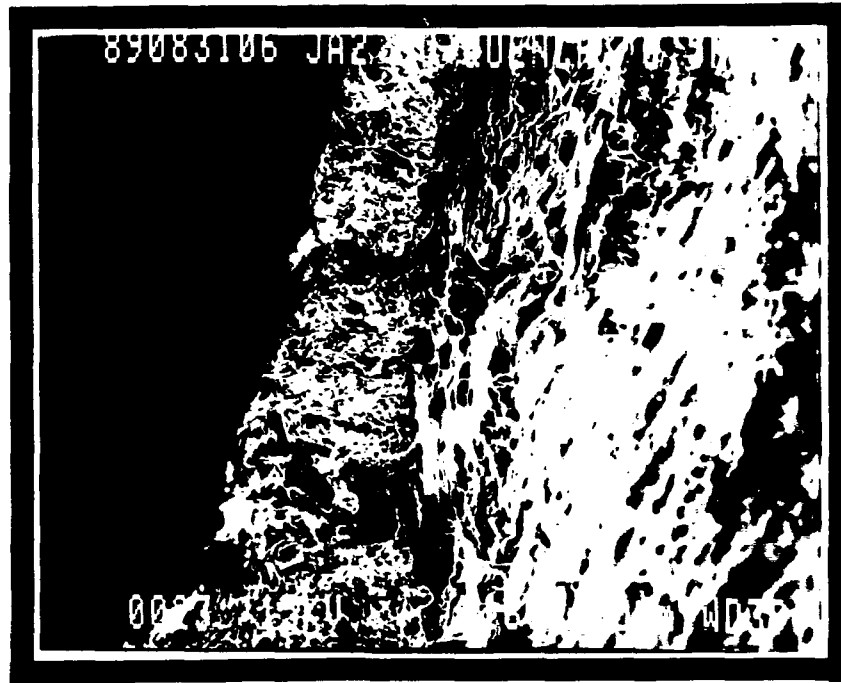
Figure 21. SEM Photograph (180x) of Cross Section of Burned Surface of JA2 (0.5 MPa, Copper Quenched).

Table 1. Compositions of Propellant Formulations Studied

Propellant	Composition	Percentage
XM39	RDX	76.00
	Cellulose Acetate Butyrate (CAB)	12.00
	Acetyl Triethyl Citrate (ATEC)	7.60
	Nitrocellulose (NC) (12.6% N)	4.00
	Ethyl Centralite (EC)	0.40
HMX2	HMX	80.00
	Polyester (PE)	20.00
M30	Nitroguanidine (NQ)	47.70
	Nitrocellulose (NC) (12.68% N)	28.00
	Nitroglycerine (NG)	22.50
	Ethyl Centralite (EC)	1.50
	Cryolite	0.30
JA2	Nitrocellulose (NC) (13.04% N)	59.50
	Nitroglycerine (NG)	14.90
	Diethylene Glycol Dinitrate (DEGDN)	24.80
	Ethyl Centralite (EC)	0.70
	Magnesium Oxide	0.05
	Graphite	0.05

Table 2. HPLC Chromatographic Area Ratios for RDX, HMX, and Nitrosoamine Peaks

Sample		Area Percentages (Area Ratios × 100)			
		NHMX?/HMX	DRDX/RDX	MRDX/RDX	HMX/RDX
XM39	WQ	17.4	0.6	3.70	7.5
HMX2	WQ	0.5			
HMX2	WQ	0.6			
XM39	Unburned	0.0	0.0	0.00	7.0
XM39	WQ	21.6	1.1	5.80	8.6
HMX2	WQ	1.4			
HMX2	Unburned	0.0			
RDX	WQ	1.6	0.0	0.05	4.1
RDX	WQ	1.4	0.0	0.30	9.4
RDX	WQ	0.0	0.0	0.30	10.5
RDX	Unburned	0.0	0.0	0.00	5.3
RDX	Unburned	0.0			
RDX	WQ, FM	4.3	0.2	3.00	12.7
RDX	WQ, FM	3.9	0.6	6.80	27.2
XM39	WQ	13.8	0.5	3.50	13.5
XM39	SE, 1.0 MPa	0.0	0.2	1.70	—
XM39	SE, 1.0 MPa	0.0	0.9	6.20	9.7
XM39	SE, 1.0 MPa	3.2	0.8	2.30	10.7
XM39	Unburned	0.0	0.0	0.00	6.1
XM39	Unburned	0.0	0.0	0.00	7.7
XM39	1.0 MPa, CQ	5.8	1.3	4.40	10.8
XM39	2.0 MPa, CQ	0.0	0.0	0.80	9.6
XM39	2.0 MPa, CQ	0.0	0.0	1.10	8.3
XM39	Unburned	0.0	0.0	0.00	7.6
XM39	1.0 MPa, CQ	5.9	0.5	4.90	11.7
RDX	0.5 MPa, CQ	2.1	0.0	0.90	8.9
RDX	0.25 MPa, CQ	0.7	0.0	1.30	7.5
RDX	Unburned	0.0			
RDX	Unburned	0.0	0.0	0.00	6.1
HMX2	0.5 MPa, CQ	3.6			
HMX2	1.0 MPa, CQ	0.0			
HMX2	2.0 MPa, CQ	0.0			
HMX2	Unburned	0.0			
HMX2	Unburned	0.0			
HMX2	Unburned	0.0			

WQ = Burned-layer scrapings from a grain burned in air at atmospheric pressure and quenched in water.
FM = Foamy material thrown off by burning RDX (1 At of air, water quench).
SE = Burned-layer scrapings from a grain that self-extinguished while burning in a strand burner at 1.0 MPa.
CQ = Burned-layer scrapings from a grain burned in a strand burner at the indicated pressure (0.25, 0.5, 1.0, or 2.0 MPa) with conductive quenching by the copper mounting block.

Table 3. Stabilizer and Plasticizer Peak Areas and Ratios From Burned Surface and From Unburned XM39

| | | Areas | | |
Sample		Stabilizer	Plasticizer	Ratio (×100)
XM39	Unburned	219.00	8.580	3.9
XM39	Unburned	65.20	2.550	3.9
XM39	WQ	77.00	0.000	0.0
XM39	WQ	186.00	0.000	0.0
XM39	WQ	133.00	0.000	0.0
XM39	WQ	147.00	2.400	1.6
XM39	WQ	225.00	0.881	0.4
XM39	Unburned	90.00	3.890	4.3
XM39	1.0 MPa, SE	125.00	2.930	2.3
XM39	1.0 MPa, SE	46.40	0.000	0.0
XM39	1.0 MPa, SE	117.00	2.340	2.0
XM39	1.0 MPa, SE	146.00	1.310	0.9
XM39	Unburned	121.00	5.590	4.6
XM39	Unburned	206.00	9.390	4.6
XM39	Unburned	65.90	2.110	3.2
XM39	1.0 MPa, CQ	27.20	0.436	1.6
XM39	1.0 MPa, CQ	95.00	2.220	2.3
XM39	2.0 MPa, CQ	498.30	23.000	4.6
XM39	2.0 MPa, CQ	280.00	11.600	4.1
XM39	2.0 MPa, CQ	195.00	8.030	4.1
XM39	2.0 MPa, CQ	105.00	3.380	3.2
XM39	2.0 MPa, CQ	204.00	7.940	3.9
XM39	2.0 MPa, CQ	92.30	2.760	3.0
XM39	2.0 MPa, CQ	115.00	3.800	3.3
XM39	1.0 MPa, SE	85.10	1.960	2.3
XM39	2.0 MPa, CQ	69.10	2.040	3.0
XM39	1.0 MPa, SE	45.60	0.640	1.4
XM39	2.0 MPa, CQ	171.71	5.820	3.4
XM39	2.0 MPa, CQ	85.80	2.590	3.0
XM39	1.0 MPa, SE	69.90	1.990	2.8
XM39	2.0 MPa, CQ	98.80	2.740	2.8
XM39	1.0 MPa, SE	95.20	3.370	3.5
XM39	1.0 MPa, SE	104.00	2.140	2.0
XM39	2.0 MPa, CQ	99.40	4.340	4.4
XM39	Unburned	241.00	11.900	4.9
XM39	Unburned	152.00	6.820	4.5
XM39	Unburned	63.60	2.120	3.3
XM39	2.0 MPa, CQ	47.90	1.310	2.7
XM39	2.0 MPa, CQ	75.00	2.330	3.1

WQ = Burned-layer scrapings from a grain burned in air at atmospheric pressure and quenched in water.
SE = Burned-layer scrapings from a grain that self-extinguished while burning in a strand burner at 1.0 MPa.
CQ = Burned-layer scrapings from a grain burned in a strand burner at the indicated pressure (0.5, 1.0, or 2.0 MPa) with conductive quenching by the copper mounting block.

Table 4. Miscellaneous Unknown Peaks (Not Present in Unburned Samples) in HPLC
Chromatograms of Burned Samples of XM39, HMX2, RDX, M30, and JA2

Sample	Pressure	Quench	Retention Time (min) of Unknown Peaks
XM39	(Unburned) Ambient 0.5–2.0 MPa	— Water Copper	— 1.0, 1.2 1.2, 2.0
HMX2	(Unburned) Ambient 0.5–2.0 MPa	— Water Copper	— 1.0, 1.1, 1.8 1.0, 1.4, 2.2
RDX	(Unburned) Ambient 0.25–0.5 MPa	— Water Copper	— 1.2 Not Examined
M30	(Unburned) Ambient 0.5–2.0 MPa	— Water Copper	— 1.0, 1.2 1.4
JA2	(Unburned) Ambient 0.5–2.0 MPa	— Water Copper	— 1.2, 1.8 1.2

Table 5. Unknown Peaks in GCMS Chromatograms of Burned Samples of XM39, HMX2, RDX, M30, and JA2

Sample	Pressure	Quench	Retention Time (min) of Unknown Peaks
XM39	(Unburned) Ambient 0.5–2.0 MPa	— Water Copper	5.3,[a] 6.1,[b] 11.0[c] 4.1,[d] 5.3,[e] 6.1,[b] 8.1,[f,g] 11.0,[c] 16.6[g,h]
HMX2	(Unburned) Ambient 0.5–2.0 MPa	— Water Copper	— — —
RDX	(Unburned) Ambient 0.25–0.5 MPa	— Water Copper	— — —
M30	(Unburned) Ambient 0.5–2.0 MPa	— Water Copper	— 6.1[i] 6.1[i]
JA2	(Unburned) Ambient 0.5–2.0 MPa	— Water Copper	— — —

[a] The mass spectrum of this peak included m/e 60, 27, 73, 42, 41, 43, 45, 38, 29, 26, 15, 31, 38, 40, 44, and 55.

[b] The mass spectrum of this peak included m/e 43, 30, 15, 88, and 58.

[c] This peak appears to be due to the following two different compounds: 1) m/e 57, 43, 71, 85, 29, 41, 42, 55, and 56; and 2) 29, 112, 139, 212, 27, 84, 213, 167, 39, 140, 138, 214, 185, 184, 157, 156, 128, 113, 85, 83, 69, 67, 66, 57, 55, 53, 45, 44, 43, 42, 41, 38, 31, 30, 26, and 15.

[d] The mass spectrum of this peak included m/e 43, 87, 42, 15, 29, 41, 39, 72, 59, 58, and 61.

[e] The mass spectrum of this peak included m/e 55, 43, 83, 98, 60, 39, 29, 15, 41, 42, and 53.

[f] The mass spectrum of this peak included m/e 95, 81, 41, 55, 39, 152, 67, 69, 83, 43, 109, 108, 93, 82, 79, 77, 68, 53, 51, 44, 42, 24, 12, and 11.

[g] Present only in self-extinguished samples.

[h] The mass spectrum of this peak included m/e 149 (by far the most intense), 29, 41, 76, 104, 223, 150, 39, 205, 56, 151, 122, 121, 105, 93, 77, 75, 65, 57, 55, 51, 50, 44, 43, 42, 40, 39, 30, 28, 19, 18, 16, 15, and 11.

[i] The mass spectrum of this peak included m/e 43, 30, 15, 88, 58, 29, and 100.

Table 6. Summary of Observation From SEM Examination of Quenched Propellant and Composition Samples

Sample	Conditions	Melt-Layer Thickness (μm)	Description of Surface
XM39	Water Quench Ambient (Air)	100–300	Bubbles, crystallization; molten binder.
	Copper Quench		
	0.5 MPa		Did not burn
	1.0 MPa	< 100	Bubbles, crystallization; decomposed binder (?) overlying RDX.
	2.0 MPa	30–100	Similar to 1.0 MPa.
HMX2	Water Quench	~ 25–100	Bubbles, crystallization; solidified binder (?); melt layer is poorly defined due to large particle size.
	Copper Quench		
	0.5 MPa	~ 10–75	Same as ambient.
	1.0 MPa		Similar to 0.5 MPa.
	2.0 MPa	~ 10–75	Similar to 1.0 MPa.
RDX	Water Quench Ambient (Air)	~ 100–200	Smooth surface, surprisingly few bubbles or signs of crystallization; many humps on surface (subsurface bubbles?).
	Copper Quench		
	0.25 MPa	present; otherwise unobservable	Considerable crystallization.
	0.5 MPa	present; otherwise unobservable	Considerable crystallization.
M30	Water Quench Ambient (Air)	5–10	Very thin liquid layer (bubbles); objects up to 1 mm across (polymeric decomposition products?) are scattered across surface.
	Copper Quench		
	0.5 MPa	0–10	Similar but fewer objects; fewer, larger bubbles and signs of crystallization (or ends of original, unburned NQ crystals?) between bubbles.
	1.0 MPa	0–10	Similar to 0.5-MPa sample.
	2.0 MPa	0–5	Similar to 1.0-MPa sample.
JA2	Water Quench Ambient (Air)	< 5	Some samples show signs of bubbles, others show no signs of crystallization, although surface appears somewhat cracked and uneven; objects up to ca 0.25 mm are scattered over the burned surface.
	Copper Quench		
	0.5 MPa	< 5	Similar but less cracked and uneven; bubbles scattered over burned surface.
	1.0 MPa	< 5	Similar but less cracked and uneven; bubbles scattered over burned surface.
	2.0 MPa	< 5	Similar to 1.0 MPa except fewer, smaller bubbles and more protrusions (unbroken bubbles?).

INTENTIONALLY LEFT BLANK.

7. REFERENCES

Behrens, R., Jr. "Thermal Decomposition of HMX in the Condensed Phase." Proceedings of the 26th JANNAF Combustion Meeting, CPIA Publication 529, vol. 1, p. 39, October 1989.

Cohen-Nir, E. "Combustion Characteristics of Advanced Nitramine-Based Propellants." The 18th Symposium (International) on Combustion, The Combustion Institute, pp. 195–206, 1981.

Cohen, N. S., B. B. Stokes, and L. D. Strand. "Mechanistic Study of Plateau Behavior in High Energy Propellants. Part II: Effects of Propellant Formulation and Pressure on Extinguished Surfaces." Proceedings of the 26th JANNAF Combustion Meeting, CPIA Publication 529, vol. 3, pp. 21–38, October 1989.

Derr, R. L., and T. L. Boggs. "Role of Scanning Electron Microscopy in the Study of Solid Propellant Combustion. Part III: The Surface Structure and Profile Characteristics of Burning Composite Solid Propellants." Combustion Science and Technology, vol. 1, pp. 369–384, 1970.

Derr, R. L., T. L. Boggs, D. E. Zurn, and E. J. Dibble. "The Combustion Characteristics of HMX." Proceedings of the 11th JANNAF Combustion Meeting, CPIA Publication 261, vol. 1, pp. 231–241, December 1974.

Fifer, R. A. "Chemistry of Nitrate Ester and Nitramine Propellants." Fundamentals of Solid Propellant Combustion, edited by K. K. Kuo and M. Summerfield, American Institute of Aeronautics and Astronautics, New York, chap. 4, pp. 177–237 (see p. 186), 1984.

Fifer, R. A., S. A. Liebman, P. J. Duff, K. D. Fickie, and M. A. Schroeder. "Thermal Degradation Mechanisms of Nitramine Propellants." Proceedings of the 22nd JANNAF Combustion Meeting, CPIA Publication 432, vol. 2, pp. 537–546, October 1985.

Gordon, A. J., and R. A. Ford. The Chemist's Companion. New York: John Wiley and Sons, p. 194, 1972.

Hoffsommer, J. C., and D. J. Glover. "Thermal Decomposition of 1,3,5-Trinitro-1,3,5-Triazacyclohexane (RDX): Kinetics of Nitroso Intermediates Formation." Combustion and Flame, vol. 59, pp. 303–10, 1985.

Hoffsommer, J. C., D. J. Glover, and W. L. Elban. "Quantitative Evidence for Nitroso Compound Formation in Drop-Weight Impacted RDX Crystals." Journal of Energetic Materials, vol. 3, pp. 149–167, 1985.

Kubota, N. "Combustion Mechanisms of Nitramine Composite Propellants." The 18th Symposium (International) on Combustion, The Combustion Institute, pp. 187–194, 1981.

Kubota, N., and S. Sakamoto. "Combustion Mechanisms of HMX." Propellants, Explosives, and Pyrotechnics, vol. 14, pp. 6–11, 1989.

Lee, P. R., and M. H. Back. "Kinetic Studies of the Thermal Decomposition of Nitroguanidine Using Accelerating Rate Calorimetry." Thermochimica Acta, vol. 127, pp. 89–100, 1988.

Mansour, A. N., J. Sharma, and G. B. Wilmot. "X-ray Absorption (XANES and EXAFS) Study of Lead Catalyst in the Condensed Phase Combustion Zone of Double-Base Rocket Propellants." Proceedings of the 22nd JANNAF Combustion Meeting, CPIA Publication 432, vol. 2, pp. 41–51, Pasadena, CA, October 1985.

Novikov, S. S., and Y. S. Ryzantsev. "Extinction of Propellant Near the Contact With a Metal." AIAA Journal, vol. 8, pp. 358–359, 1970.

Rauch, F. C., and W. P. Colman. "Studies on Composition B." Contract DAAA 21-68-C-0334, American Cyanamid Company, Stamford, CT, March 1970. (AD 869226)

Schroeder, M. A., R. A. Fifer, M. S. Miller, and R. A. Pesce-Rodriguez. "Condensed-Phase Processes During Solid Propellant Combustion. Part I: Preliminary Chemical and Microscopic Examination of Extinguished Propellant Samples." Proceedings of the 26th JANNAF Combustion Meeting, CPIA Publication 529, vol. 3, pp. 329–343, Pasadena, CA, October 1989.

Schroeder, M. A., R. A. Fifer, M. S. Miller, and R. A. Pesce-Rodriguez. "Condensed-Phase Processes During Solid Propellant Combustion. Part I: Preliminary Chemical and Microscopic Examination of Extinguished Propellant Samples." BRL-MR-3845, U.S. Army Ballistic Research Laboratory, Aberdeen Proving Ground, MD, June 1990.

Sharma, J., and B. C. Beard. "Fundametals of X-ray Photoelectron Spectroscopy (XPS) and Its Applications to Explosives and Propellants." Chemistry and Physics of Energetic Materials, edited by S. Bulusu, NATO ASI Series, vol. 309C, pp. 569–585, Norwell, MA: Kluwer Academic Publishers, 1990a.

Sharma, J., and B. C. Beard. "X-ray Study of Hot Spots and Sensitization Centers in Energetic Materials." Chemistry and Physics of Energetic Materials, edited by S. Bulusu, NATO ASI Series, vol. 309C, pp. 587–603, Norwell, MA: Kluwer Academic Publishers, 1990b.

Sharma, J., F. Santiago, G. B. Wilmot, and R. A. Campolattaro. "XPS Study of Catalyst Atoms in Double-Base Rocket Propellant Catalyzed by Lead Salt Burning Rate Modifier." Proceedings of the 19th JANNAF Combustion Meeting, CPIA Publication 366, vol. 2, pp. 1–6, Greenbelt, MD, October 1982.

Sharma, J., G. B. Wilmot, R. A. Campolattaro, and F. Santiago. "XPS Study of Condensed Phase Combustion in Double-Base Rocket Propellant With and Without Lead Salt Burning Rate Modifier." Proceedings of the 21st JANNAF Combustion Meeting, CPIA Publication 412, vol. 2, pp. 173–182, Laurel, MD, October 1984.

Sharma, J., G. B. Wilmot, A. A. Campolattaro, and F. Santiago. "XPS Study of Condensed Phase Combustion in Double-Base Rocket Propellant With and Without Lead Salt Burning Rate Modifier." Combustion and Flame, vol. 85, pp. 416–426, 1991.

34

Silverstein, R. M., G. C. Bassler, and T. C. Morrill. <u>Spectrometric Indentification of Organic Compounds</u>. New York: John Wiley and Sons, p. 169, 1981.

Stals, J., and M. J. Pitt. "Investigations of the Thermal Stability of Nitroguanidine Below Its Melting Point." <u>Australian Journal of Chemistry</u>, vol. 28, pp. 2629–2640, 1975.

Stokes, B. B., R. H. Taylor, Jr., N. S. Cohen, and D. L. Zurn. "Mechanistic Study of Plateau Behavior in High Energy Propellants. Part I: Burn Rate Curves and Combustion Data at 10 MPa." <u>Proceedings of the 26th JANNAF Combustion Meeting</u>, CPIA Publication 529, vol. 3, pp. 1–20, October 1989.

Vanderhoff, J. A. "Spectral Emission and Absorption Studies of Solid Propellant Combustion." <u>Proceedings of the 25th JANNAF Combustion Meeting</u>, CPIA Publication 498, vol. 4, pp. 537–547, October 1988.

Wilmot, G. B., E. G. Powell, J. Sharma, and D. Carlson. "Combustion Mechanisms of Lead-Salt-Catalyzed Double-Base Propellants." <u>Proceedings of the 18th JANNAF Combustion Meeting</u>, CPIA Publication 347, vol. 3, pp. 297–306, October 1981.

Zhao, B., and Z. Zhao. "High Pressure Combustion Characteristics of RDX-Based Propellants." <u>The 22nd Symposium (International) on Combustion</u>, The Combustion Institute, pp. 1835–1842, 1988.

Zimmer-Galler, R. "Correlations Between Deflagration Characteristics and Surface Properties of Nitramine-Based Propellants." <u>AIAA Journal</u>, vol. 6, pp. 2107–2110, 1968.

INTENTIONALLY LEFT BLANK.

2   Administrator
Defense Technical Info Center
ATTN: DTIC-DDA
Cameron Station
Alexandria, VA 22304-6145

1   Commander
U.S. Army Materiel Command
ATTN: AMCAM
5001 Eisenhower Ave.
Alexandria, VA 22333-0001

1   Commander
U.S. Army Laboratory Command
ATTN: AMSLC-DL
2800 Powder Mill Rd.
Adelphi, MD 20783-1145

2   Commander
U.S. Army Armament Research,
Development, and Engineering Center
ATTN: SMCAR-IMI-I
Picatinny Arsenal, NJ 07806-5000

2   Commander
U.S. Army Armament Research,
Development, and Engineering Center
ATTN: SMCAR-TDC
Picatinny Arsenal, NJ 07806-5000

1   Director
Benet Weapons Laboratory
U.S. Army Armament Research,
Development, and Engineering Center
ATTN: SMCAR-CCB-TL
Watervliet, NY 12189-4050

(Unclass. only)1   Commander
U.S. Army Armament, Munitions,
and Chemical Command
ATTN: AMSMC-IMF-L
Rock Island, IL 61299-5000

1   Director
U.S. Army Aviation Research
and Technology Activity
ATTN: SAVRT-R (Library)
M/S 219-3
Ames Research Center
Moffett Field, CA 94035-1000

1   Commander
U.S. Army Missile Command
ATTN: AMSMI-RD-CS-R (DOC)
Redstone Arsenal, AL 35898-5010

1   Commander
U.S. Army Tank-Automotive Command
ATTN: ASQNC-TAC-DIT (Technical
Information Center)
Warren, MI 48397-5000

1   Director
U.S. Army TRADOC Analysis Command
ATTN: ATRC-WSR
White Sands Missile Range, NM 88002-5502

1   Commandant
U.S. Army Field Artillery School
ATTN: ATSF-CSI
Ft. Sill, OK 73503-5000

2   Commandant
U.S. Army Infantry School
ATTN: ATZB-SC, System Safety
Fort Benning, GA 31903-5000

(Class. only)1   Commandant
U.S. Army Infantry School
ATTN: ATSH-CD (Security Mgr.)
Fort Benning, GA 31905-5660

(Unclass. only)1   Commandant
U.S. Army Infantry School
ATTN: ATSH-CD-CSO-OR
Fort Benning, GA 31905-5660

1   WL/MNOI
Eglin AFB, FL 32542-5000

Aberdeen Proving Ground

2   Dir, USAMSAA
ATTN: AMXSY-D
AMXSY-MP, H. Cohen

1   Cdr, USATECOM
ATTN: AMSTE-TC

3   Cdr, CRDEC, AMCCOM
ATTN: SMCCR-RSP-A
SMCCR-MU
SMCCR-MSI

1   Dir, VLAMO
ATTN: AMSLC-VL-D

10   Dir, USABRL
ATTN: SLCBR-DD-T

No. of Copies	Organization	No. of Copies	Organization
1	HQDA (SARD-TC, C.H. Church) WASH DC 20310-0103	4	Commander Naval Surface Warfare Center ATTN: B. Beard, R-34 R. Bernecker, R-13 J. Sharma, R-34 G.B. Wilmot, R-16 Silver Spring, MD 20903-5000
4	Commander US Army Research Office ATTN: R. Ghirardelli D. Mann R. Singleton R. Shaw P.O. Box 12211 Research Triangle Park, NC 27709-2211	5	Commander Naval Research Laboratory ATTN: M.C. Lin J. McDonald E. Oran J. Shnur R.J. Doyle, Code 6110 Washington, DC 20375
4	Commander US Army Armament Research, Development, and Engineering Center ATTN: SMCAR-AEE-WW, S. Bulusu SMCAR-AEE-WE, T. Chen SMCAR-AEE-B, D.S. Downs SMCAR-AEE, J.A. Lannon Picatinny Arsenal, NJ 07806-5000	1	Commanding Officer Naval Underwater Systems Center Weapons Dept. ATTN: R.S. Lazar/Code 36301 Newport, RI 02840
1	Commander US Army Armament Research, Development, and Engineering Center ATTN: SMCAR-AEE-BR, L. Harris Picatinny Arsenal, NJ 07806-5000	4	Commander Naval Weapons Center ATTN: A. Atwood, Code 3981 T. Boggs, Code 388 K. Kraeutle, Code 388 T. Parr, Code 3895 China Lake, CA 93555-6001
2	Commander US Army Missile Command ATTN: AMSMI-RD-PR-E, A.R. Maykut AMSMI-RD-PR-P, R. Betts Redstone Arsenal, AL 35898-5249	1	Superintendent Naval Postgraduate School Dept. of Aeronautics ATTN: D.W. Netzer Monterey, CA 93940
1	Office of Naval Research Department of the Navy ATTN: R.S. Miller, Code 432 800 N. Quincy Street Arlington, VA 22217	3	AL/LSCF ATTN: R. Corley R. Geisler J. Levine Edwards AFB, CA 93523-5000
1	Commander Naval Air Systems Command ATTN: J. Ramnarace, AIR-54111C Washington, DC 20360	1	AFOSR ATTN: J.M. Tishkoff Bolling Air Force Base Washington, DC 20332
1	Commander Naval Surface Warfare Center ATTN: J.L. East, Jr., G-23 Dahlgren, VA 22448-5000	1	OSD/SDIO/IST ATTN: L. Caveny Pentagon Washington, DC 20301-7100

1 Commandant
   USAFAS
   ATTN: ATSF-TSM-CN
   Fort Sill, OK 73503-5600

1 F.J. Seiler Research Laboratory
   Directorate of Chemical Sciences
   FJSRL/NC (AFSC)
   ATTN: S.A. Shackleford
   USAF Academy, CO 80840-6528

1 University of Dayton Research Institute
   ATTN: D. Campbell
   AL/PAP
   Edwards AFB, CA 93523

1 NASA
   Langley Research Center
   Langley Station
   ATTN: G.B. Northam/MS 168
   Hampton, VA 23365

5 National Bureau of Standards
   ATTN: J. Hastie
          M. Jacox
          T. Kashiwagi
          H. Semerjian
          W. Tsang
   US Department of Commerce
   Washington, DC 20234

1 Aerojet Solid Propulsion Co.
   ATTN: P. Micheli
   Sacramento, GA 95813

1 Applied Combustion Technology, Inc.
   ATTN: A.M. Varney
   P.O. Box 607885
   Orlando, FL 32860

2 Applied Mechanics Reviews
   The American Society of
    Mechanical Engineers
   ATTN: R.E. White
          A.B. Wenzel
   345 E. 47th Street
   New York, NY 10017

1 Atlantic Research Corp.
   ATTN: R.H.W. Waesch
   7511 Wellington Road
   Gainesville, VA 22065

1 AVCO Everett Research
    Laboratory Division
   ATTN: D. Stickler
   2385 Revere Beach Parkway
   Everett, MA 02149

1 Battelle
   ATTN: TACTEC Library, J. Huggins
   505 King Avenue
   Columbus, OH 43201-2693

1 Cohen Professional Services
   ATTN: N.S. Cohen
   141 Channing Street
   Redlands, CA 92373

1 Exxon Research & Eng. Co.
   ATTN: A. Dean
   Route 22E
   Annandale, NJ 08801

1 General Applied Science
    Laboratories, Inc.
   77 Raynor Avenue
   Ronkonkama, NY 11779-6649

1 General Electric Ordnance
    Systems
   ATTN: J. Mandzy
   100 Plastics Avenue
   Pittsfield, MA 01203

1 General Motors Rsch Labs
   Physical Chemistry Department
   ATTN: T. Sloane
   Warren, MI 48090-9055

2 Hercules, Inc.
   Allegheny Ballistics Lab.
   ATTN: W.B. Walkup
          E.A. Yount
   P.O. Box 210
   Rocket Center, WV 26726

1 Alliant Techsystems, Inc.
   Marine Systems Group
   ATTN: D.E. Broden/
          MS MN50-2000
   600 2nd Street NE
   Hopkins, MN 55343

No. of Copies	Organization	No. of Copies	Organization
1	Alliant Techsystems, Inc. ATTN: R.E. Tompkins MN38-3300 5700 Smetana Drive Minnetonka, MN 55343	2	Princeton Combustion Research Laboratories, Inc. ATTN: M. Summerfield N.A. Messina 475 US Highway One Monmouth Junction, NJ 08852
1	IBM Corporation ATTN: A.C. Tam Research Division 5600 Cottle Road San Jose, CA 95193	1	Hughes Aircraft Company ATTN: T.E. Ward 8433 Fallbrook Avenue Canoga Park, CA 91303
2	IIT Research Institute ATTN: R.F. Remaly A. Snelson 10 West 35th Street Chicago, IL 60616	1	Rockwell International Corp. Rocketdyne Division ATTN: J.E. Flanagan/HB02 6633 Canoga Avenue Canoga Park, CA 91304
2	Director Lawrence Livermore National Laboratory ATTN: C. Westbrook M. Costantino P.O. Box 808 Livermore, CA 94550	5	Director Sandia National Laboratories ATTN: R. Cattolica, Div. 8354 S. Johnston, Div. 8354 P. Mattern, Div. 8354 R. Skocypec, Div. 1513 D. Stephenson, Div. 8354 Livermore, CA 94550
1	Lockheed Missiles & Space Co. ATTN: George Lo 3251 Hanover Street Dept. 52-35/B204/2 Palo Alto, CA 94304	1	Science Applications, Inc. ATTN: R.B. Edelman 23146 Cumorah Crest Woodland Hills, CA 91364
1	Director Los Alamos National Lab ATTN: B. Nichols, T7, MS-B284 P.O. Box 1663 Los Alamos, NM 87545	3	SRI International ATTN: G. Smith D. Crosley D. Golden D. McMillen 333 Ravenswood Avenue Menlo Park, CA 94025
1	National Science Foundation ATTN: A.B. Harvey Washington, DC 20550	1	Stevens Institute of Tech. Davidson Laboratory ATTN: R. McAlevy, III Hoboken, NJ 07030
1	Olin Ordnance ATTN: V. McDonald, Library P.O. Box 222 St. Marks, FL 32355-0222	1	Sverdrup Technology, Inc. LERC Group ATTN: R.J. Locke, MS SVR-2 2001 Aerospace Parkway Brook Park, OH 44142
1	Paul Gough Associates, Inc. ATTN: P.S. Gough 1048 South Street Portsmouth, NH 03801-5423		

No. of Copies	Organization	No. of Copies	Organization
1	Sverdrup Technology, Inc. ATTN: J. Deur 2001 Aerospace Parkway Brook Park, OH 44142	1	California Institute of Technology ATTN: F.E.C. Culick/ MC 301-46 204 Karman Lab. Pasadena, CA 91125
1	Thiokol Corporation Elkton Division ATTN: S.F. Palopoli P.O. Box 241 Elkton, MD 21921	1	University of California Los Alamos Scientific Lab. P.O. Box 1663, Mail Stop B216 Los Alamos, NM 87545
3	Thiokol Corporation Wasatch Division ATTN: S.J. Bennett P.O. Box 524 Brigham City, UT 84302	1	University of California, Berkeley Chemistry Deparment ATTN: C. Bradley Moore 211 Lewis Hall Berkeley, CA 94720
1	United Technologies Research Center ATTN: J. Stufflebeam, MS 129-90 A.C. Eckbreth East Hartford, CT 06108	1	University of California, San Diego ATTN: F.A. Williams AMES, B010 La Jolla, CA 92093
3	United Technologies Corp. Chemical Systems Division ATTN: R.S. Brown T.D. Myers (2 copies) P.O. Box 49028 San Jose, CA 95161-9028	2	University of California, Santa Barbara Quantum Institute ATTN: K. Schofield M. Steinberg Santa Barbara, CA 93106
1	Universal Propulsion Company ATTN: H.J. McSpadden Black Canyon Stage 1 Box 1140 Phoenix, AZ 85029	1	University of Colorado at Boulder Engineering Center ATTN: J. Daily Campus Box 427 Boulder, CO 80309-0427
1	Veritay Technology, Inc. ATTN: E.B. Fisher 4845 Millersport Highway P.O. Box 305 East Amherst, NY 14051-0305	2	University of Southern California Dept. of Chemistry ATTN: S. Benson C. Wittig Los Angeles, CA 90007
1	Brigham Young University Dept. of Chemical Engineering ATTN: M.W. Beckstead Provo, UT 84058		
1	California Institute of Tech. Jet Propulsion Laboratory ATTN: L. Strand/MS 512/102 4800 Oak Grove Drive Pasadena, CA 91109	1	Cornell University Department of Chemistry ATTN: T.A. Cool Baker Laboratory Ithaca, NY 14853

No. of
Copies   Organization

1   University of Delaware
     ATTN: T. Brill
     Chemistry Department
     Newark, DE   19711

1   University of Florida
     Dept. of Chemistry
     ATTN: J. Winefordner
     Gainesville, FL   32611

3   Georgia Institute of Technology
     School of Aerospace Engineering
     ATTN: E. Price
              W.C. Strahle
              B.T. Zinn
     Atlanta, GA   30332

1   University of Illinois
     Dept. of Mech. Eng.
     ATTN: H. Krier
     144MEB, 1206 W. Green St.
     Urbana, IL   61801

1   Johns Hopkins University/APL
     Chemical Propulsion
       Information Agency
     ATTN: T.W. Christian
     Johns Hopkins Road
     Laurel, MD   20707

1   University of Michigan
     Gas Dynamics Lab
     Aerospace Engineering Bldg.
     ATTN: G.M. Faeth
     Ann Arbor, MI   48109-2140

1   University of Minnesota
     Dept. of Mechanical
       Engineering
     ATTN: E. Fletcher
     Minneapolis, MN   55455

3   Pennsylvania State University
     Applied Research Laboratory
     ATTN: K.K. Kuo
              H. Palmer
              M. Micci
     University Park, PA   16802

No. of
Copies   Organization

1   Pennsylvania State University
     Dept. of Mechanical Engineering
     ATTN: V. Yang
     University Park, PA   16802

1   Polytechnic Institute of NY
     Graduate Center
     ATTN: S. Lederman
     Route 110
     Farmingdale, NY   11735

2   Princeton University
     Forrestal Campus Library
     ATTN: K. Brezinsky
              I. Glassman
     P.O. Box 710
     Princeton, NJ   08540

1   Purdue University
     School of Aeronautics
       and Astronautics
     ATTN: J.R. Osborn
     Grissom Hall
     West Lafayette, IN   47906

1   Purdue University
     Department of Chemistry
     ATTN: E. Grant
     West Lafayette, IN   47906

2   Purdue University
     School of Mechanical
       Engineering
     ATTN: N.M. Laurendeau
              S.N.B. Murthy
     TSPC Chaffee Hall
     West Lafayette, IN   47906

1   Rensselaer Polytechnic Inst.
     Dept. of Chemical Engineering
     ATTN: A. Fontijn
     Troy, NY   12181

1   Stanford University
     Dept. of Mechanical
       Engineering
     ATTN: R. Hanson
     Stanford, CA   94305

INTENTIONALLY LEFT BLANK.

USER EVALUATION SHEET/CHANGE OF ADDRESS

This laboratory undertakes a continuing effort to improve the quality of the reports it publishes. Your comments/answers below will aid us in our efforts.

1. Does this report satisfy a need? (Comment on purpose, related project, or other area of interest for which the report will be used.) _____

_____

_____

2. How, specifically, is the report being used? (Information source, design data, procedure, source of ideas, etc.) _____

_____

_____

3. Has the information in this report led to any quantitative savings as far as man-hours or dollars saved, operating costs avoided, or efficiencies achieved, etc? If so, please elaborate. _____

_____

_____

4. General Comments. What do you think should be changed to improve future reports? (Indicate changes to organization, technical content, format, etc.) _____

_____

_____

BRL Report Number _____ Division Symbol _____

Check here if desire to be removed from distribution list. ____

Check here for address change. ____

Current address: Organization _____

Address _____

_____

DEPARTMENT OF THE ARMY
Director
U.S. Army Ballistic Research Laboratory
ATTN: SLCBR-DD-T
Aberdeen Proving Ground, MD 21005-5066

OFFICIAL BUSINESS

| | NO POSTAGE NECESSARY IF MAILED IN THE UNITED STATES |

BUSINESS REPLY MAIL
FIRST CLASS PERMIT No 0001, APG, MD

Postage will be paid by addressee.

Director
U.S. Army Ballistic Research Laboratory
ATTN: SLCBR-DD-T
Aberdeen Proving Ground, MD 21005-5066